Federal State Autonomous Educational Institution of Higher Education
«Moscow Institute of Physics and Technology (National Research University)»
Landau Phystech School of Physics and Research
Chair for «Problems in theoretical physics»

Institute for Theoretical Physics L.D. Landau (Russian Academy of Sciences)

Major of study: 03.04.01 Applied Mathematics and Physics
Academic specialization: General and applied physics

MULTIFRACTALLY-ENHANCED SUPERCONDUCTIVITY IN TWO-DIMENSIONAL SYSTEMS WITH SPIN-ORBIT COUPLING

(Master's thesis)

Student:
Andriyakhina Elizaveta Sergeevna

Scientific supervisor:
Prof. Dr. Burmistrov Igor Sergeevich

Moscow 2023

Annotation

This master's thesis presents a detailed investigation into the enhancement of superconductivity in two-dimensional systems, particularly emphasizing the role of multifractality and spin-orbit coupling. The study is based on the understanding that Anderson localization and electron-electron interactions can enhance superconductivity due to the multifractality of electron wave functions.

The primary contribution of this work is the development of a theoretical model for multifractally-enhanced superconducting states in two-dimensional systems in the presence of spin-orbit coupling. Utilizing the Finkel'stein nonlinear sigma model, we have derived modified Usadel and gap equations that account for renormalizations due to the interplay of disorder and interactions. We find energy dependence of the superconducting spectral gap, which is influenced by multifractal correlations. We have determined the superconducting transition temperature and the superconducting spectral gap for both Ising and strong spin orbit couplings. Additionally, we have analyzed mesoscopic fluctuations of the local density of states in the superconducting state, finding that spin-orbit coupling reduces the amplitude of these fluctuations. Finally, this thesis explores the interaction-renormalized Usadel equation beyond the lowest order limit in interaction constants. Its behavior near the critical temperature is examined.

Contents

Acknowledgments

I want to express my heartfelt gratitude to my supervisor, Prof. Dr. Igor Burmistrov, for his invaluable guidance and mentorship during my master's program, and for sharing his valuable scientific experience with me.

I am also incredibly thankful to my friends and family for their exceptional support throughout my academic journey. I would like to extend a special thanks to D.E. Kiselov, S.S. Babkin, and K.G. Nazaryan for always being ready to brainstorm scientific problems and for their valuable contributions to improving my scientific communication skills.

ESA and Prof. Dr. Igor Burmistrov are grateful to C. Brun, T. Cren, F. Evers, I. Gornyi, M. Lizee, A. Mirlin, P. Nosov, S. Raghu, and M. Stosiek for collaboration on related projects and useful discussions. The research is partially supported by the Russian Foundation for Basic Research (Grant No. 20-52-12013) and by the Basic Research Program of HSE.

Introduction

Superconductivity and Anderson localization are two fundamental quantum phenomena that continue to attract significant interest.

The concept of Anderson localization, first introduced by P. W. Anderson in 1958 [1], describes the absence of diffusion in a disordered system due to wave interference. In a disordered medium, an electron can be localized, meaning its wave function decays exponentially with distance from a given point, instead of spreading out across the system.

The localization of the wave function is described by its exponential decay away from a given point:

$$|\psi(\boldsymbol{r})|^2 \propto e^{-|\boldsymbol{r}-\boldsymbol{r}_0|/\xi_{\text{loc}}}$$

where $\psi(\boldsymbol{r})$ is the wave function at a point $\boldsymbol{r}$, $\boldsymbol{r}_0$ is the position of the localized state, and ξ_{loc} is the localization length.

On the other hand, quasiparticle interactions in metals play a crucial role in understanding many-body phenomena such as superconductivity. These interactions can be categorized into different channels based on the spin and orbital symmetries of the interacting quasiparticles. Given a generic interaction potential between particles, we can divide these terms into small-frequency momentum scattering within particle-particle (hole-hole) and particle-hole interactions, or into spin-singlet and spin-triplet contributions.

Within this research and in accordance with [2], singlet and triplet channels are terms used to describe the particle-hole interaction channel, which involves small frequency-momentum transfers between a particle and a hole. In the singlet channel, the total spin of the two interacting quasiparticles is zero. While in the triplet channel, the total spin of the two interacting quasiparticles is one.

The particle-particle or Cooper interaction channel refers to the exchange of small energy and momentum between two particles or two holes. The interaction leads to the formation of Cooper pairs, which are pairs of quasiparticles with opposite momenta and spins. [1]

[1] In our research, we examine a pointlike interaction. Despite the potential triplet term in the Cooper channel, it vanishes for an instantaneous, pointlike interaction due to the Pauli principle. However, in some materials, spin fluctuations can induce an attractive force in the triplet channel [3, 4].

Before we proceed, let us also discuss the importance of spin-orbit coupling in superconducting materials. Spin-orbit coupling impacts superconductivity in various ways. It can induce unconventional superconductivity, modify pairing symmetry and gap structure, influence vortex behavior, and even give rise to topological superconductivity (for a review, see [5]). While these effects are interesting and complex on their own, in this research, we focus solely on the impact of spin relaxation on the scaling properties of superconductivity. I emphasize that throughout this thesis, I exclusively consider s-wave pairing and assume a homogeneous gap that is independent of direction.

Let's discuss the various mechanisms of spin relaxation and their effects on quasiparticle interactions. Spin-orbit coupling introduces an additional term to the Hamiltonian, see [2]:

$$H_{so} = -i\alpha\boldsymbol{\sigma} \cdot [\nabla(v_{so}(\boldsymbol{r}) + u_{so}(\boldsymbol{r})) \times \nabla],$$

where the spin-orbit interaction in the absence of impurities is denoted as $v_{so}(\boldsymbol{r})$, and $u_{so}(\boldsymbol{r})$ represents the impurities-induced component. The parameter α represents the spin-orbit coupling constant, and $\boldsymbol{\sigma}$ is a Pauli matrix vector that corresponds to spin-1/2. It should be noted that both terms, $u_{so}(\boldsymbol{r})$ and $v_{so}(\boldsymbol{r})$, contribute to spin relaxation and result in finite spin-flip times. The specific details of the mechanism can lead to anisotropic spin relaxation, characterized by times $\tau_{\text{so}}^{(x)}$, $\tau_{\text{so}}^{(y)}$, and $\tau_{\text{so}}^{(z)}$ for scattering of the x, y, and z components, respectively.

In the case where impurities-induced contribution is the main source of spin-orbit coupling and the sample is two-dimensional, see [6], the description of the spin-orbit coupling (in momentum space) can be expressed as the random term $u_{so}(\boldsymbol{p} \times \boldsymbol{p}')$, where $\boldsymbol{p}$ and $\boldsymbol{p}'$ represent the momenta before and after scattering, respectively. Note that since $\boldsymbol{p}$ and $\boldsymbol{p}'$ lie in a plane of a superconductor, only the σ^z component survives and leads to a finite scattering time

$$1/\tau_{\text{so}}^{(z)} = \pi\nu\langle u_{so}(\boldsymbol{p} \times \boldsymbol{p}')^2\rangle, \quad 1/\tau_{\text{so}}^{(x)} = 1/\tau_{\text{so}}^{(y)} = 0.$$

Thus, in this case, one gapless triplet mode corresponding to $S^z = 0$ is implemented. At length scales much larger than the spin-orbit length $L_{so}^{(imp)} = \sqrt{D\tau_{\text{so}}^{(z)}}$, where D is the diffusion coefficient and $\tau_{\text{so}}^{(z)}$ is the relaxation time for the z-component, the massive triplet modes become effectively frozen. We would like

to emphasize that the pathway leading to one gapless triplet mode is not singular. Another significant pathway is the so-called Ising spin-orbit coupling [7], particularly relevant for transition metal dichalcogenides (TMDs) – ultra-thin superconductors. These materials have recently been widely studied experimentally. To underscore the potential of a multifractal mechanism amplifying superconductivity in TMDs, we refer to the instance of a single massless mode as the Ising spin orbit.

On the other hand, if intrinsic spin-orbit coupling is important, it can result in finite values for $1/\tau_{\rm so}^{(x,y)}$ through the D'yakonov-Perel' (DP) spin relaxation mechanism [8]. The DP mechanism operates based on the concept that the spin of a carrier rotates around an effective magnetic field determined by the carrier's momentum, which arises from the spin-orbit interaction. When the carrier undergoes scattering due to impurities or phonons, its momentum changes, altering the direction of the effective magnetic field. If these scattering events occur frequently enough, the carrier's spin can become randomized, leading to spin relaxation. The relaxation rates for the triplet modes are determined by $1/\tau_{\rm so}^{(x,y,z)} \sim \Delta_{so}^2\tau$, where Δ_{so} represents the spin-orbit splitting and τ is the momentum relaxation time. As a result, the triplet modes, whether diffusons or cooperons, are suppressed at length scales $L \gg L_{so}^{(DP)} = v_F/\Delta_{so}$.

Summing up, we are considering a spin-orbit interaction that is weak enough to preserve the symmetry of the gap (s-wave), but strong enough that the critical length $L_{T_c} \sim \sqrt{D/T_c}$, where T_c is the superconductor critical temperature, is significantly larger than $\min(L_{so}^{(imp)}, L_{so}^{(DP)})$. While it is recognized that spin-orbit coupling can result in mixed singlet and triplet pairings, see [9], in the clean limit, we propose that in the presence of disorder, the unconventional pairing component will be disrupted following a similar mechanism described by the Abrikosov-Gorkov theory. Furthermore, we adopt a perspective in which the broadening of the quasiparticle spectrum caused by disorder significantly outweighs the splitting induced by spin-orbit interaction, i.e. $\tau\Delta_{so} \ll 1$. Therefore, we do not anticipate any lifting of spin degeneracy or triplet pairing.

When the aforementioned spin relaxation mechanisms compete, different regimes can arise. Let's discuss which cases are realized based on the strength of the spin-orbit interaction. There are two characteristic lengths associated with the spin-orbit interaction, $L_{so}^{(imp)}$ and $L_{so}^{(DP)}$, and the length scale associated with superconductivity L_{T_c}. If $L_{T_c} \ll \min(L_{so}^{(imp)}, L_{so}^{(DP)})$, we effectively have a spin rotation

symmetric case where all modes can be treated as gapless. If L_{T_c} lies in the range $L_{so}^{(imp)} \ll L_{T_c} \ll L_{so}^{(DP)}$, only the $S^z = 0$ triplet mode remains gapless. Finally, if $L_{T_c} \gg L_{so}^{(DP)}$, all triplet modes are suppressed.

Note also that the system can exhibit different localization regimes depending on the presence and type of spin-orbit relaxation. In the absence of spin-orbit coupling, it is in a weak-localization regime. When spin-orbit coupling suppresses relaxation in all directions, the system enters a weak anti-localization regime. Finally, when only one triplet mode is gapless, the system exists in a regime where the conductivity remains nearly constant with changes in sample size. Let us now return to the interplay of disorder and interaction in 2D superconductors.

Initially, it was believed that non-magnetic disorder does not affect the s-wave superconducting order parameter, a concept known as the "Anderson theorem" [10, 11, 12]. However, this paradigm later shifted to view superconductivity and disorder as antagonists due to Anderson localization [1]. Strong localization was predicted to suppress superconductivity [13, 14, 15, 16]. A similar destruction of superconductivity was predicted due to the Coulomb interaction at weak disorder [17, 18, 19, 20, 21, 22, 23]. The experimental discovery of the superconductor-to-insulator transition [24] has further stimulated interest in the effects of disorder on superconducting correlations in thin films (see Refs. [25, 26, 27] for a review).

Recently, there has been a paradigm shift in our understanding of superconductivity. Predictions made in Refs. [28, 29] suggest that Anderson localization can lead to an enhancement of the superconducting transition temperature, T_c, for systems near the Anderson transition (e.g., in three dimensions). This mechanism is based on the multifractal behavior of wave functions - a well-known companion of Anderson localization - that leads to an enhancement of effective attraction between electrons. This mechanism operates in the absence of long-ranged Coulomb repulsion. Later, the multifractal enhancement of T_c was predicted for systems in the regime of weak localization (or anti-localization), which is relevant for weakly disordered superconducting films [30, 31]. These analytical predictions have been further tested by numerical computations for the disordered attractive Hubbard model on a two-dimensional lattice [32, 33, 34]. Recently, an observed increase in T_c with increasing disorder in monolayer niobium dichalcogenides [35, 36] has been suggested as a demonstration of the multifractal-enhancement mechanism.

One approach to characterizing the multifractally-enhanced superconducting state involves studying the mesoscopic fluctuations of the local density of states

[37, 38]. This could potentially be very promising due to (i) the numerous reported tunneling spectroscopy data on point-to-point fluctuations of the local density of states in thin superconducting films [39, 40, 41, 42, 43, 44], and (ii) a qualitative agreement between the theory [45] developed for temperatures $T > T_c$ and experiments on the local density of states in the normal phase of disordered superconducting films.

However, there are examples of superconducting thin films and two-dimensional systems with broken spin rotational symmetry due to the presence of spin-orbit coupling. This includes systems such as single atomic layers of Pb on Si [46], $SrTiO_3$ surfaces [47, 48], $LaAlO_3/SrTiO_3$ interfaces [49, 50], and MoS_2 flakes [51, 52, 53]. Moreover, the existence of Ising-type spin-orbit coupling is anticipated in monolayer niobium dichalcogenides, where multifractal enhancement of superconductivity has been measured [35, 36]. This necessitates the development of a theory that can account for the multifractal enhancement of superconductivity in two-dimensional systems with spin-orbit coupling.

In this work, we extend the theory of the multifractal superconducting state developed in Ref. [37] to thin films with spin-orbit coupling. Similar to Ref. [37], our focus is on the case of weak short-ranged electron-electron interaction [2]. We consider an intermediate disorder strength where the renormalization group analysis for the normal state predicts a parametrically enhanced T_c compared to the conventional Bardeen-Cooper-Schrieffer (BCS) result [30]. Using the Finkel'stein nonlinear sigma model, we derive the Usadel equation and the equation for the spectral gap function. These equations are modified due to the interplay of disorder and interactions at scales shorter than the superconducting coherence length. We solve these equations for the cases of Ising-type and strong spin-orbit couplings. In the Ising case, a single triplet diffusive mode remains effective at long length scales, while in the strong spin-orbit coupling case, all triplet modes are suppressed. In both cases, we determine the superconducting transition temperature and investigate the energy dependence of the spectral gap function at low temperatures ($T \ll T_c$) and near the transition ($T_c - T \ll T_c$). We find that the maximum magnitude of the gap is proportional to T_c, indicating its enhancement due to multifractality. Additionally, we estimate the mesoscopic fluctuations of the local density of states. Despite the absence of spin rotational symmetry, we

[2] The long-range component (Coulomb) of the interaction can be suppressed in films covered by a substrate with a high dielectric constant.

find that these fluctuations exhibit logarithmic divergence with the system size (if the effect of dephasing is neglected).

The outline of the thesis is as follows. In Sec. 1, we present the general scheme for the description of the superconducting state. This scheme is applied to the case of Ising-type spin-orbit coupling in Sec. 2. In Sec. 3, we consider the case of strong spin-orbit coupling. The results of the sections listed were published in [54]. We also include additional developments beyond the lower-order perturbation theory in Sec. 5. The thesis is concluded with a summary and conclusions in Sec. 6. Some technical details are delegated to the Appendices.

1 Equation for the spectral gap

In dirty superconductors, there is a significant energy window between the diffusive scale of $1/\tau$ (where τ represents the mean free time) and the energy scale associated with superconductivity, which can be chosen as T_c. To accurately describe the superconducting properties at the energy scale T_c (with the corresponding length scale being the superconducting coherence length, $\xi = \sqrt{D/T_c}$), it is necessary to account for the interaction effects among the diffusive modes within the energy interval $T_c \lesssim \varepsilon \lesssim 1/\tau$.

Similar to studies of normal dirty metals, the interaction of diffusive modes leads to the renormalization of physical parameters in the superconducting state, such as conductance and interaction strengths. These renormalizations have a significant impact on the Usadel equation and the self-consistency equation for the spectral gap. To derive these modified equations, we employ the nonlinear sigma model approach described in Ref. [37] (see Appendix A for details). This procedure yields the following modified Usadel equation for the spectral angle θ_ε:

$$\frac{D_\varepsilon}{2}\nabla^2\theta_\varepsilon - |\varepsilon|\sin\theta_\varepsilon + \Delta_\varepsilon\cos\theta_\varepsilon = 0. \tag{1.1}$$

Here $\varepsilon = \pi T(2n+1)$ denotes fermionic Matsubara frequency. Equation (1.1) differs from the standard Usadel equation [55] by energy dependent spectral gap Δ_ε and energy dependent diffusion coefficient D_ε [3].

To the lowest order in disorder and interaction, the spectral gap satisfies the following equation

$$\begin{aligned}\Delta_\varepsilon =& -2\pi T\sum_{\varepsilon_n'>0}\sin\theta_{\varepsilon'}\left\{\gamma_c - 2\frac{(\gamma_s-\mathcal{N}\gamma_t)}{g}\int\frac{d^2\boldsymbol{q}}{(2\pi)^2}\frac{D}{Dq^2+E_\varepsilon+E_{\varepsilon'}}\right\},\\ E_\varepsilon =& |\varepsilon|\cos\theta_\varepsilon + \Delta\sin\theta_\varepsilon.\end{aligned} \tag{1.2}$$

Here, $\gamma_c < 0$, γ_s, and γ_t represent the bare values of the dimensionless interaction amplitudes in the Cooper channel, as well as in the singlet and triplet particle-hole channels, respectively. We presume the interaction in the particle-hole channel to be weak and short-ranged. Consequently, we examine the case where $|\gamma_{c,s,t}| \ll 1$.

[3] In this thesis we are interested in the superconducting state which is spatially homogeneous on the scale of the order of ξ. Therefore, we shall not discuss energy dependence of the diffusion coefficient here.

The disorder is regulated by the bare dimensionless (in units e^2/h) conductance $g = h/(e^2 R_\square)$, where $R_\square$ is the film resistance per square in the normal state. The bare diffusion coefficient D is linked with conductance and the density of states, ν, at the Fermi energy in the normal state via the Einstein relation $g = 2\pi\nu D$. The superconducting order parameter Δ establishes the bare value of the superconducting gap.

Parameter $\mathcal{N}$ in Eq. (1.2) counts the number of massless triplet diffusive modes. We will focus on the cases $\mathcal{N} = 0$ and 1 whereas the case $\mathcal{N} = 3$ was considered in Ref. [37].

We note that a similar form of the self-consistency equation for the spectral gap has been derived in Ref. [56, 57] in the case of Coulomb interaction ($\gamma_s = -1$) and neglect of exchange interaction ($\gamma_t = 0$) by means of the diagrammatic technique.

Equation (1.2) resembles the standard self-consistency equation in the BCS theory except for the logarithmic renormalization of the attraction interaction parameter γ_c. This renormalization is identical to that in the normal metal, except the infrared scale is set by $\max \varepsilon, \varepsilon', \Delta$. The perturbative result (1.2) for the renormalization of γ_c can be extended via the renormalization group technique, as seen in Ref. [37] for details.

Then, by solving the modified Usadel equation (1.1) as $\sin\theta_\varepsilon = \Delta_\varepsilon/\sqrt{\varepsilon^2 + \Delta_\varepsilon^2}$, we find the following self-consistency relation for Δ_ε:

$$\Delta_\varepsilon = -2\pi T \sum_{\varepsilon'>0} \frac{\gamma_c \left(L_{E_\varepsilon + E_{\varepsilon'}}\right) \Delta_{\varepsilon'}}{\sqrt{\varepsilon'^2 + \Delta_{\varepsilon'}^2}}, \tag{1.3}$$

Here $L_\varepsilon = \sqrt{D/\varepsilon}$ is the diffusive length associated with the energy scale ε. The flow of γ_c with the length scale L is governed by the following renormalization group equation (see Ref. [37] for $\mathcal{N} = 3$),

$$\frac{d\gamma_c}{dy} = -\frac{t}{2}(\gamma_s - \mathcal{N}\gamma_t). \tag{1.4}$$

Here $y = \ln L/\ell$ with ℓ and L being the mean free path and the system size, respectively. The dimensionless resistance is denoted as $t = 2/(\pi g)$. Its bare value t_0 is assumed to be small, $t_0 \ll 1$.

Equation (1.4) does not contain the standard term, -γ_c^2, which is responsible for the Cooper instability in the clean case. This term is encoded in the super-

conducting order parameter Δ (see Ref. [37] for details).

It is tempting to replace Δ with Δ_ε in the expression for E_ε in Eq. (1.3) to make it a fully self-consistent equation for Δ_ε. This was done in Ref. [37] based on the relation between the Usadel equation, linearized in variation of θ_ε, and the Cooperon propagator with coinciding energies. However, further analysis shows that the Cooperon propagator with two non-equal Matsubara energies has a more complex structure after renormalization.[4] Fortunately, as we will see below, the precise form of the difference $E_\varepsilon - |\varepsilon|$ is not critical for the results reported in this thesis.

Eq. (1.4) needs to be supplemented by renormalization group equations for $\gamma_{s,t}$ and t. However, their exact form depends on the magnitude of $\mathcal{N}$. We will analyze Eq. (1.3) separately for the cases $\mathcal{N} = 0$ and 1. Moving forward, we assume that the bare values of interaction and disorder are weak: $|\gamma_{s0}|, |\gamma_{t0}|, |\gamma_{c0}|, t_0 \ll 1$.

[4]The author is grateful to P. Nosov for this comment.

2 $\mathcal{N} = 1$: Ising Spin-Orbit Coupling

In this section, our focus is on superconducting films with Ising spin-orbit coupling. In this case, the in-plane spin-flip scattering rates induced by spin-orbit coupling are smaller than the out-of-plane rate, i.e., $1/\tau_{\rm so}^{x,y} \ll 1/\tau_{\rm so}^{z}$. As a result, one triplet diffusive mode, corresponding to the total spin projection $S_z = 0$, remains gapless, along with all singlet diffusive modes. This scenario leads to the realization of the case $\mathcal{N} = 1$ for the Ising spin-orbit coupling.

To analyze the gap equation (1.3), it is necessary to determine the actual dependence of γ_c on the length scale. In Ref. [31], the complete set of one-loop renormalization group equations for $\gamma_{s,t,c}$ and t was derived using the background field renormalization of the nonlinear sigma model above the superconducting transition temperature. By applying the same method in the superconducting state, we obtain:

$$\frac{dt}{dy} = -\frac{t^2}{2}(\gamma_s + \gamma_t + 2\gamma_c), \tag{2.1a}$$

$$\frac{d}{dy}\begin{pmatrix}\gamma_s\\ \gamma_t\\ \gamma_c\end{pmatrix} = -\frac{t}{2}\begin{pmatrix}1 & 1 & 2\\ 1 & 1 & -2\\ 1 & -1 & 0\end{pmatrix}\begin{pmatrix}\gamma_s\\ \gamma_t\\ \gamma_c\end{pmatrix}. \tag{2.1b}$$

We note that Eq. (2.1a) is valid under the assumption that $|\gamma_{s,t,c}| \ll 1$. Similar to the case of a normal metal [58], weak localization and weak antilocalization effects cancel each other out in the presence of Ising spin-orbit coupling. Eq. (2.1a) implies that the dimensionless resistance t remains nearly constant in the leading order. Therefore, we can assume $t \simeq t_0$ below. Eq. (2.1b) suggests that under the renormalization group flow, the interaction parameters approach the so-called BCS line, where $-\gamma_s = \gamma_t = \gamma_c \equiv \gamma$ [30]. To describe the system's behavior at length scales $y \gtrsim t_0^{-1}$, we project Eq. (2.1b) onto the BCS line. As a result, we work with an effective interaction parameter γ that evolves according to:

$$d\gamma/dy \simeq t_0\gamma, \quad \gamma_0 = (\gamma_{t0} - \gamma_{s0} + 2\gamma_{c0})/4 < 0. \tag{2.2}$$

Solving the above equation, we find

$$\gamma(L) = \gamma_0 (L/\ell)^{t_0}. \tag{2.3}$$

In the following, we assume that disorder dominates over the interaction, i.e., $t_0 \gg |\gamma_0|$. This regime is known to exhibit multifractal enhancement of the superconducting transition temperature [30]. The transition temperature T_c can be estimated using the relation $|\gamma(L_{T_c})| \sim t_0$ (see Appendix B). This leads to the following estimation:

$$T_c \sim (1/\tau)(|\gamma_0|/t_0)^{2/t_0}. \tag{2.4}$$

We observe that the superconducting critical temperature T_c corresponds to $y_c \sim t_0^{-1} \ln(t_0/|\gamma_0|) \gg t_0^{-1}$. This validates the projection onto the BCS line.

2.1 The Critical Temperature

More precisely, the superconducting transition temperature T_c can be determined from the linearized self-consistent equation, as given in Eq. (1.3). It should be noted that after projecting the self-consistency equation (1.3) onto the BCS line, the parameter γ_c is replaced by γ. The linearized version of the self-consistency equation can then be expressed as follows:

$$\Delta_\varepsilon = -2\pi T \sum_{\varepsilon'>0} \gamma(L_{\varepsilon+\varepsilon'}) \frac{\Delta_{\varepsilon'}}{\varepsilon'}. \tag{2.5}$$

Taking into account the actual dependence of $\gamma(L)$ on L, Eq. (2.3), we find

$$\Delta_n = \frac{|\gamma_0|}{(2\pi T\tau)^{t_0/2}} \sum_{n'\geqslant 0}^{n_{\max}} \frac{\Delta_{n'}}{(n+n'+1)^{t_0/2}(n'+1/2)}, \tag{2.6}$$

where the parameter $n_{\max} \simeq 1/(2\pi T\tau)$ serves as a natural cutoff for the number of Matsubara frequencies belonging to the diffusive regime. The search for T_c can be reformulated as a problem of finding the maximal eigenvalue of the corresponding matrix. The superconducting transition temperature satisfies the equation $(2\pi T_c\tau)^{t_0/2} = |\gamma_0|\lambda_M$, where λ_M is the maximal eigenvalue of the matrix $M_{nn'} = (n+n'+1)^{-t_0/2}(n'+1/2)^{-1}$.

By numerically solving Eq. (2.6) using the power method (see Appendix C),

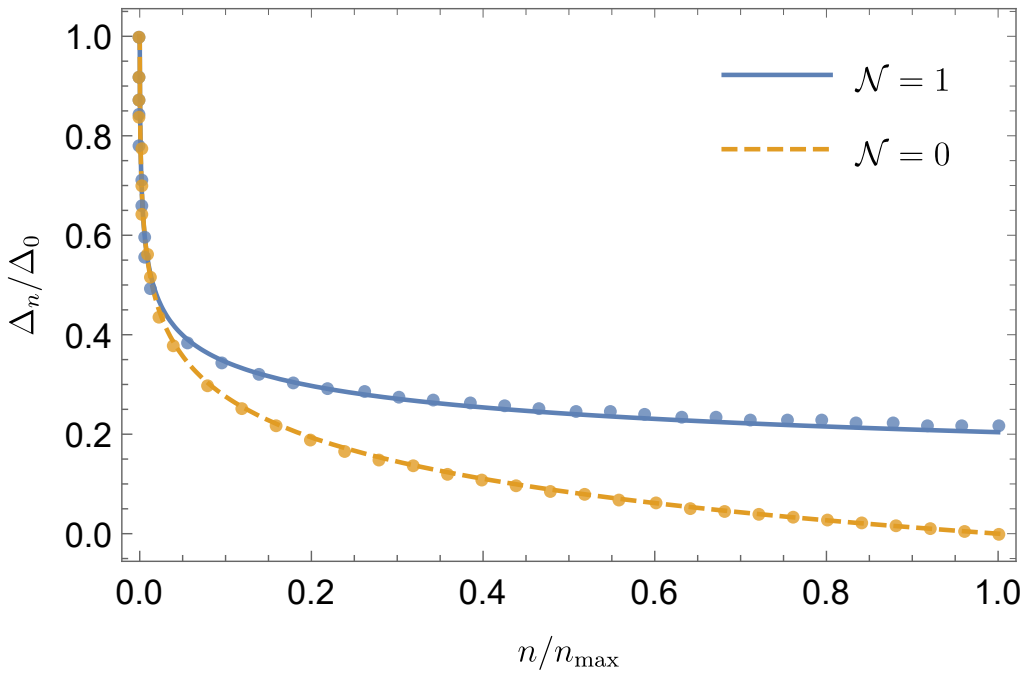

Figure 1: The dependence of the gap function Δ_n on the Matsubara energies $\varepsilon_n = 2\pi T(n+1/2)$ for T near the critical temperature T_c. Solid and dashed lines show analytical expressions (2.11) and (3.11), respectively. Dots of the corresponding colors mark numerical solutions for leading eigenvectors of Eqs. (2.6) and (3.6).

we find that $\lambda_M \simeq 1.4/t_0$, resulting in the following expression:

$$T_c \simeq \frac{1}{2\pi\tau}(1.4|\gamma_0|/t_0)^{2/t_0}. \tag{2.7}$$

The right eigenvector r_n of the matrix M corresponding to λ_M is depicted in Fig. 1. It is worth noting that the left eigenvector of the matrix M can be expressed as $l_n = r_n/(n+1/2)$. The spectral gap exhibits a pronounced energy dependence, which is in contrast to the BCS model where it is a constant value.

The result (2.7) can also be justified through an analytical treatment of Eq. (2.6). First, we replace $(n+n'+1)^{t_0/2}$ with $\max\{(n+1/2)^{t_0/2}, (n'+1/2)^{t_0/2}\}$, which is justified by the smallness of the exponent $t_0 \ll 1$. Then, we introduce a variable

$$u_\varepsilon = \frac{2}{t_0}|\gamma(L_\varepsilon)| = \frac{2|\gamma_0|}{t_0}(\varepsilon\tau)^{-t_0/2}. \tag{2.8}$$

Then, using the Euler-Maclaurin resummation on the right-hand side of Eq. (2.5),

we obtain

$$\Delta_{u_n} \simeq u_n \int_{u_n}^{u_0} du \frac{\Delta_u}{u} + \int_{u_\infty}^{u_n} du \Delta_u + \frac{at_0}{2} u_n \Delta_{u_0}, \tag{2.9a}$$

$$u_\infty \equiv u_{1/\tau} \sim |\gamma_0|/t_0 \ll 1, \tag{2.9b}$$

$$a = 1 + \sum_{k=1}^{\infty} 2^{2k-1} B_{2k}/k \approx 1.27. \tag{2.9c}$$

Here u_∞ corresponds to $n_{\max}$ and B_{2k} denotes even Bernoulli numbers. At $T = T_c$ we seek the solution of Eq. (2.9a) in the form $\Delta_{u_n} = \Delta_{u_0} f(u_n)$ with the normalization $f(u_0) = 1$. The integral equation (2.9a) can be reduced to the following Cauchy problem for the unknown function $f(u)$,

$$\begin{gathered} f''(u) = -f(u)/u, \\ f'(u_0) = at_0/2, \qquad f'(u_\infty) = f(u_\infty)/u_\infty. \end{gathered} \tag{2.10}$$

Solving Eq. (2.10), we obtain

$$f(u) = \frac{F_1(u)}{F_1(u_0)}, \quad F_1(u) \simeq \sqrt{u} J_1(2\sqrt{u}). \tag{2.11}$$

Here $J_1(x)$ denotes the Bessel function of the first kind. We note that for the sake of brevity in the above expression $F_1(u)$ is written in the lowest order in small parameters $|\gamma_0| \ll t_0 \ll 1$. Although one can easily find the exact solution to $f(u)$, in what follows we do not need it. We also note that the solution (2.11) satisfies the normalization condition $f(u_0) = 1$ and the boundary condition at $u = u_\infty$. The yet unknown parameter u_0 determines the superconducting transition temperature as

$$T_c = (2\pi\tau)^{-1} ((2/u_0)|\gamma_0|/t_0)^{2/t_0}. \tag{2.12}$$

The value of u_0 can be determined from the boundary condition at $u = u_0$. By using the relation $(xJ_1(x))' = xJ_0(x)$ and neglecting $at_0/2$ in the right-hand side of the equation for the boundary condition at $u = u_0$, we find $u_0 \approx (j_{0,1})^2/4 \approx 1.45$, where $j_{n,k}$ is the k-th zero of the Bessel function $J_n(x)$. The result in Eq. (2.12) is in good quantitative agreement with the numerical result in Eq. (2.7). Additionally, as shown in Figure 1, there is remarkable agreement between the

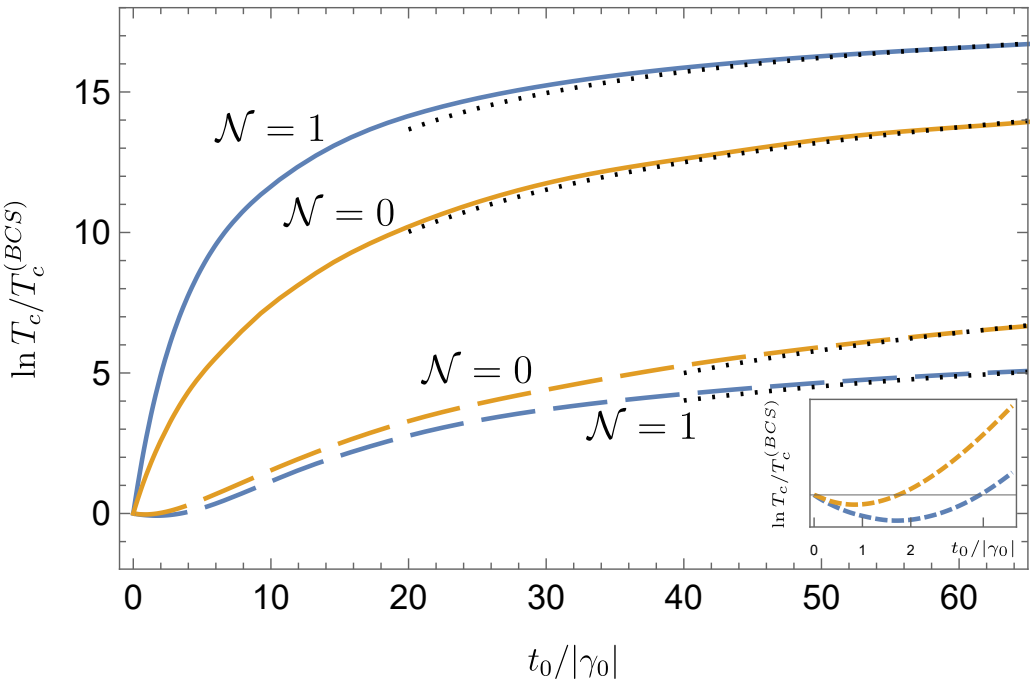

Figure 2: Multifractally-increased superconducting transition temperature T_c. Solid lines show the dependence of $\ln T_c/T_c^{(BCS)}$ on magnitude of the ratio $t_0/|\gamma_0|$, when the initial interaction parameters γ_{s0}, γ_{t0}, γ_{c0} lie on the BCS-line, i.e. $-\gamma_s = \gamma_t = \gamma_c = \gamma$ for $\mathcal{N} = 1$ and $-\gamma_s = \gamma_c = \gamma$ for $\mathcal{N} = 0$. Dashed lines of the corresponding colors illustrate the behavior of $\ln T_c/T_c^{(BCS)}$, when the initial parameters deviate from the BCS-line. This can lead to a decrease in the critical temperature T_c in comparison to $T_c^{(BCS)}$ at a small ratio of t_0 to $|\gamma_0|$ (see inset), but eventually $\ln T_c/T_c^{(BCS)}$ becomes positive and continues to grow with increasing disorder. Black dotted lines correspond to the expressions (2.12) and (3.12).

function $f(u_n)$ and the numerically computed eigenvector corresponding to the maximum eigenvalue of the matrix M.

Equation (2.7) predicts an increase in T_c with an increase in disorder t_0, at a fixed γ_0. However, Eq. (2.7) is valid only for $t_0 \gg |\gamma_0|$. To explore the behavior for various values of t_0, we numerically solve the self-consistency equation (2.6). The dependence of T_c on t_0 is shown in Figure 2. As observed, for initial conditions on the BCS line, T_c increases with an increase in t_0, eventually reaching the asymptotic expression in Eq. (2.12) (black dotted lines) for $t_0 \gg |\gamma_0|$. In the case of the system away from the BCS line initially, T_c is initially suppressed with an increase in t_0, but then starts to increase at $t_0 \gtrsim |\gamma_0|$.

We now move on to examining the behaviour of the gap function Δ_ε as a function of ε at different temperature regimes: when T is close to T_c and when

$T \ll T_c$.

2.2 The Spectral Gap Function

2.2.1 The Gap Function Near T_c

At $T = T_c$, the amplitude Δ_0 of the spectral gap function vanishes. To find the dependence of Δ_ε on energy at $T_c - T \ll T_c$, we expand the modified self-consistency equation to the third order, retrieving

$$\Delta_\varepsilon = 2\pi T \sum_{\varepsilon'>0} |\gamma(L_{\varepsilon+\varepsilon'})| \left(\frac{\Delta_{\varepsilon'}}{\varepsilon'} - \frac{\Delta_{\varepsilon'}^3}{2\varepsilon'^3} \right). \tag{2.13}$$

We note that quadratic in Δ_ε terms that originate from expansion of $\left|\gamma(L_{E_\varepsilon+E_{\varepsilon'}})\right|$ are suppressed by a small factor $t_0 \ll 1$.

Let us write $\Delta_{\varepsilon_n} = \Delta_0(T) r_n$ with the normalization $r_0 = 1$. Then Eq. (2.13) becomes

$$\lambda_M \left(\frac{T}{T_c} \right)^{\frac{t_0}{2}} r_n = \sum_{n'=0}^{n_{\max}} M_{nn'} \left[r_{n'} - \frac{\frac{\Delta_0^2(T)}{8\pi^2 T_c^2} r_{n'}^3}{(n'+1/2)^2} \right]. \tag{2.14}$$

To ensure $\Delta_0(T_c) = 0$, one needs to choose r_n as the right eigenvector of the matrix $M_{nn'}$ corresponding to its maximum eigenvalue λ_M. Then, by multiplying both sides of Eq. (2.14) with the left eigenvector $l_n = r_n/(n+1/2)$ (corresponding to λ_M) from the left, we obtain:

$$\Delta_0(T) = \left(b_{\mathcal{N}} \frac{8\pi^2}{7\zeta(3)} T_c (T_c - T) \right)^{1/2}. \tag{2.15}$$

Here the constant $b_{\mathcal{N}}$ for $\mathcal{N} = 1$ is given as

$$b_1 = \frac{7\zeta(3) t_0}{2} \frac{\sum_{n=0}^{n_{\max}} r_n^2/(n+1/2)}{\sum_{n=0}^{n_{\max}} r_n^4/(n+1/2)^3}. \tag{2.16}$$

We have chosen the normalization of b_1 in a way that the quantity $b_1 - 1$ describes the deviation from the BCS theory. However, despite the strong energy dependence of the right eigenvector, as we will demonstrate below, our approximation

shows that the difference $b_1 - 1$ is actually zero.

First of all, replacing r_n^4 with $r_0^4 = 1$ in the denominator of Eq. (2.16), we find that

$$\sum_{n=0}^{n_{\max}} \frac{r_n^4}{(n+1/2)^3} \simeq 7\zeta(3). \tag{2.17}$$

Next, in order to estimate the numerator of Eq. (2.16), we replace r_n with an analytical expression $r_n = f(u_n)$, see Eq. (2.11). Hence, we obtain

$$\sum_{n=0}^{n_{\max}} \frac{r_n^2}{n+1/2} \simeq \frac{2}{t_0}\int_0^{u_0} \frac{du}{u} f^2(u) \simeq \frac{2}{t_0}. \tag{2.18}$$

Combining all the above we restore the BCS results, $b_1 = 1$, in the limit $t_0 \ll 1$. We note that in order to compute corrections to the BSC result, $b_1 = 1$, one needs to know the precise form of dependence of the infrared cut off length scale $L_{E_\varepsilon + E_{\varepsilon'}}$ on Δ_ε and $\Delta_{\varepsilon'}$ in Eq. (1.3).

One can estimate the effect of admixture of other eigenmodes to the dependence of Δ_ε on ε. Writing $\Delta_\varepsilon = \Delta_0(T)(r_n + \sum_j s_j r_n^{(j)})$ where $r_n^{(j)}$ are the right eigenvectors of the matrix M with eigenvalues $\lambda_j < \lambda_M$, we find

$$s_j = -\frac{\lambda_j}{\lambda_M - \lambda_j}\frac{\Delta_0^2(T)}{8\pi^2 T_c^2}\frac{\sum\limits_{n=0}^{N} l_n^{(j)} r_n^3/(n+1/2)^2}{\sum\limits_{n=0}^{N} l_n^{(j)} r_n^{(j)}}. \tag{2.19}$$

Here we used orthogonality condition $\sum_n l_n^{(j)} r_n = 0$ where $l_n^{(j)}$ stands for the left eigenvector of the matrix $M_{nn'}$ corresponding to the eigenvalue λ_j. We see that the admixture of the other eigenmodes at $T_c - T \ll T_c$ is completely negligible. Therefore, the energy dependence of Δ_ε on ε at $T_c - T \ll T_c$ is essentially the same as at the transition.

2.2.2 The Gap Function at $T \ll T_c$

We begin by considering the zero-temperature limit. To analyze the behavior of the gap function at $T = 0$, we replace the summation over Matsubara frequencies with an integration over energy ε' in Eq. (1.3). There are two sources of dependence on ε' in the equation. The first is the fast dependence under the square root, and the second is the slow (almost logarithmic for $t_0 \ll 1$) depen-

dence in γ. Based on the solution for $T = T_c$, we expect the gap function Δ_ε to be a decreasing function of ε.

Let us introduce the characteristic energy scale ε_0, such that $\Delta_{\varepsilon_0} = \varepsilon_0$. The structure of the equation for Δ_ε, as given by Eq. (1.3), suggests that the gap function slightly varies from its value Δ_0 at $\varepsilon = 0$ to $\Delta_{\varepsilon_0} = \varepsilon_0$ at $\varepsilon = \varepsilon_0$. This implies that $\varepsilon_0 \sim \Delta_0$. In order to determine the precise relation between ε_0 and Δ_0, as well as the dependence of Δ_ε for $\varepsilon < \Delta_0$, one needs to know the precise dependence of the infrared length scale $L_{E_\varepsilon + E_{\varepsilon'}}$ on Δ_ε and $\Delta_{\varepsilon'}$, as given by Eq. (1.3). This complication is absent at large energies $\varepsilon \gg \Delta_\varepsilon$. As we will verify later, this condition is satisfied for energies ε that are not too close to Δ_0, i.e., for $\varepsilon \gtrsim \Delta_0$, due to the smallness of the dimensional resistance $t_0 \ll 1$.

At $\varepsilon \gg \Delta_\varepsilon$ we approximate the self-consistent equation (1.3) as follows

$$\Delta_\varepsilon \simeq |\gamma(L_\varepsilon)| \int_0^{\Delta_0} \frac{d\varepsilon' \Delta_0}{\sqrt{\varepsilon'^2 + \Delta_0^2}} + |\gamma(L_\varepsilon)| \int_{\Delta_0}^{\varepsilon} \frac{d\varepsilon' \Delta_{\varepsilon'}}{\sqrt{\varepsilon'^2 + \Delta_{\varepsilon'}^2}} + \int_{\varepsilon}^{1/\tau} \frac{d\varepsilon' \Delta_{\varepsilon'}}{\sqrt{\varepsilon'^2 + \Delta_{\varepsilon'}^2}} |\gamma(L_{\varepsilon'})|. \tag{2.20}$$

Substituting Δ_ε for $\Delta_{u_\varepsilon} = \Delta_{u_0} f(u_\varepsilon)$, where u_ε is defined in Eq. (2.8), the above equation can be rewritten in the following differential form

$$f''(u_\varepsilon) = -\frac{\varepsilon f(u_\varepsilon)/u_\varepsilon}{\sqrt{\varepsilon^2 + \Delta_0^2 f^2(u_\varepsilon)}}. \tag{2.21}$$

Since we are working in the regime $\varepsilon \gg \Delta_\varepsilon$, we can safely neglect the term with Δ_0 under the square root in the right hand side of Eq. (2.21). Then Eq. (2.21) reduces to Eq. (2.10) with the same boundary conditions except $a = (1)$ now. Thus the solution can be read from Eq. (2.11). Altogether we find the following solution for the spectral gap function

$$\Delta_\varepsilon \simeq \Delta_0 \begin{cases} 1, & \varepsilon \lesssim \Delta_0, \\ F_1(u_\varepsilon)/F_1(u_{\Delta_0}), & \varepsilon \gtrsim \Delta_0. \end{cases} \tag{2.22}$$

Now we can check the assumption $\varepsilon \gg \Delta_\varepsilon$. Using Eq. (2.22), we find that

$$\frac{\varepsilon}{\Delta_\varepsilon} = \frac{u_{\Delta_0}^{2/t_0} F_1(u_{\Delta_0})}{u_\varepsilon^{2/t_0} F_1(u_\varepsilon)} \gg 1 \tag{2.23}$$

holds for all ε except close vicinity of $|\varepsilon - \Delta_0| \sim \Delta_0$.

We note perfect matching of both asymptotic results (2.22) at $\varepsilon = \Delta_0$. Using the boundary condition $f'(u_{\Delta_0}) = 0$ we find that Δ_0 coincides with T_c upto numerical prefactor,

$$\Delta_0 \sim T_c. \tag{2.24}$$

However, as we noted above our approach does not applicable in the vicinity of the point $\varepsilon = \Delta_0$. Therefore, we cannot determine the precise constant for the ratio for Δ_0/T_c. We emphasize that the dependence of the spectral gap function at $\varepsilon \gg \Delta_0$ for $T = 0$ is exactly the same as for T close to T_c.

We emphasize that the spectral gap function is parametrically enhanced at small energies. Using Eq. (2.22) we find that the spectral gap at $\varepsilon \sim 1/\tau$ (which coincides with the order parameter Δ) is proportional to $\Delta_0|\gamma_0|/t_0 \ll \Delta_0$. Typical behaviour of Δ_ε is illustrated in Fig. 3.

At non-zero temperature, the form of the spectral gap function remains the same but there is reduction of the magnitude of Δ_0 while temperature increases. At $T \ll \Delta_0$ the dependence of Δ_0 on temperature can be estimated as follows. At $\varepsilon \gg \Delta_0$ the gap function Δ_ε satisfies equation similar to Eq. (2.20) in which Δ_0 is substituted by $\Delta_0(T)$ and

$$\begin{aligned}\int\limits_0^{\Delta_0} \frac{d\varepsilon' \Delta_0}{\sqrt{\varepsilon'^2 + \Delta_0^2}} \to 2\pi T \sum_{\varepsilon'>0} \frac{\Delta_0(T)}{\sqrt{\varepsilon'^2 + \Delta_0^2(T)}} - \int\limits_{\Delta_0(T)}^{1/\tau} \frac{d\varepsilon' \Delta_0(T)}{\sqrt{\varepsilon'^2 + \Delta_0^2(T)}} \\ \simeq \int\limits_0^{\Delta_0(T)} \frac{d\varepsilon' \Delta_0(T)}{\sqrt{\varepsilon'^2 + \Delta_0^2(T)}} - \sqrt{\frac{2\pi T}{\Delta_0}} e^{-\Delta_0/T}.\end{aligned} \tag{2.25}$$

Such modification of Eq. (2.20) results in change of the constant a in the boundary conditions in Eq. (2.10). Now it becomes $a = (1) - \sqrt{2\pi T/\Delta_0}\exp(-\Delta_0/T)$. Taking this temperature shift of the constant a into account, we find

$$\Delta_0 - \Delta_0(T) \sim \sqrt{2\pi T \Delta_0}\, e^{-\Delta_0/T}, \quad T \ll \Delta_0. \tag{2.26}$$

We note that since this result is obtained with the help of the boundary condition at $\varepsilon = \Delta_0(T)$, we cannot unambiguously determine a numerical factor in Eq. (2.26).

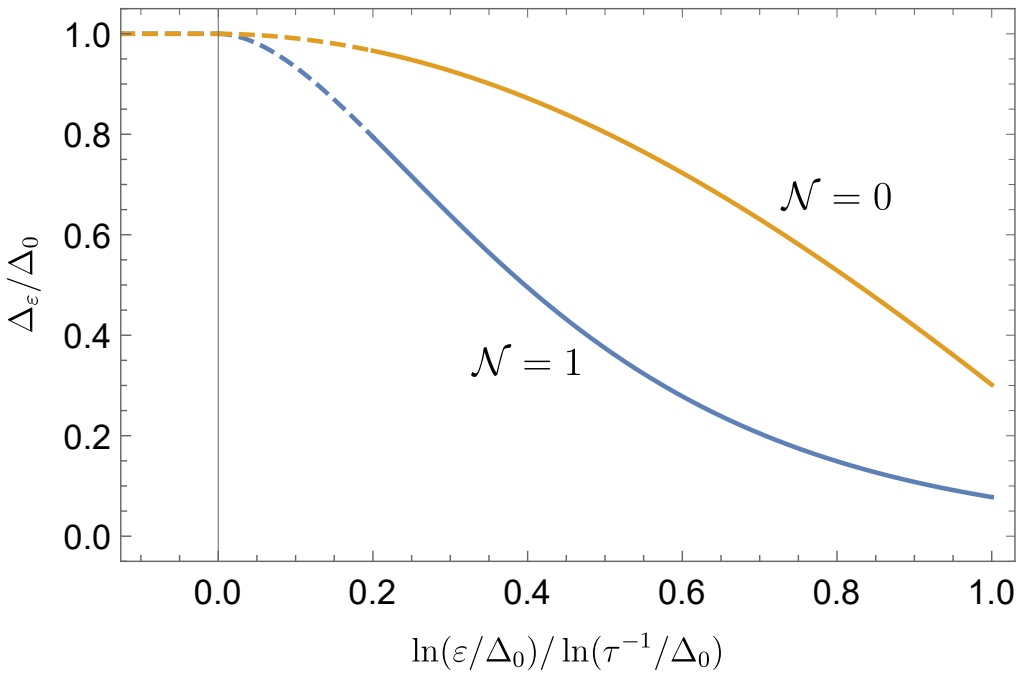

Figure 3: The dependence of the gap function Δ_ε at low temperatures on energy ε (see text). Dimensionless interaction constant is chosen to be $|\gamma_0| = 0.005$ and dimensionless resistance is $t_0 = 0.2$. Bottom curve illustrates the behaviour of Δ_ε for the case of Ising spin-orbit coupling ($\mathcal{N} = 1$) while the top one corresponds to the case of strong spin-orbit coupling ($\mathcal{N} = 0$).

3 $\mathcal{N} = 0$: Strong Spin-Orbit Coupling

In this section, we consider the case when all three spin-flip rates, $1/\tau_{\rm so}^{x,y,z}$, induced by the spin-orbit coupling, are of the same order. In this scenario, only the diffusive modes corresponding to the total spin zero remain gapless. As a result, the number of triplet modes reduces to zero, i.e., $\mathcal{N} = 0$.

For $\mathcal{N} = 0$ the renormalization group flow of the interaction parameters $\gamma_{s,c}$ and the dimensionless resistance t is governed by the following equations [31]

$$\frac{dt}{dy} = -t^2(1 + \gamma_s + 2\gamma_c)/2, \tag{3.1a}$$

$$\frac{d}{dy}\begin{pmatrix}\gamma_s\\ \gamma_c\end{pmatrix} = -\frac{t}{2}\begin{pmatrix}1 & 2\\ 1 & 0\end{pmatrix}\begin{pmatrix}\gamma_s\\ \gamma_c\end{pmatrix}. \tag{3.1b}$$

We emphasize that contrary to the case $\mathcal{N} = 1$ there is the weak-antilocalization correction (term with unity in the brackets in the right hand side of Eq. (3.1a)) that results in flow of t towards zero. In what follows we neglect terms proportional to $\gamma_{s,c}$ (Altshuler-Aronov and density-of-states-type corrections) in Eq. (3.1a) in

comparison with weak antilocalization. In accordance with Eq. (3.1b), the interaction parameters flow approaching the BCS line $-\gamma_s = \gamma_c \equiv \gamma$. Projecting Eq. (3.1b) onto the BCS line, we find

$$d\gamma/dy = t\gamma/2, \quad \gamma_0 = (2\gamma_{c0} - \gamma_{s0})/3 < 0. \tag{3.2}$$

Here γ_0 is the initial value of the effective attraction. We assume $t_0 \gg |\gamma_0|$. Solving Eqs. (3.1a) and (3.2), we obtain

$$t(L) = \frac{t_0}{1 + (t_0/2)\ln L/\ell}, \qquad \gamma(L) = \gamma_0 \frac{t_0}{t(L)}. \tag{3.3}$$

The effective attraction is growing with increase of the length scale. The superconducting critical temperature can be estimated from the condition $|\gamma(L_{T_c})| \sim t(L_{T_c})$ (see Appendix B). It results in the estimate [30]

$$\ln 1/(T_c\tau) \sim \frac{1}{\sqrt{|\gamma_0|t_0}}. \tag{3.4}$$

We note that the numerical factor cannot be determined reliably in this way.

3.1 The Critical Temperature

Let us now solve the self-consistent equation (2.5) in order to determine the superconducting transition temperature. It is convenient to introduce a parametrization of the critical temperature in the following form:

$$T_c = (2\pi\tau)^{-1} \exp\left(4/t_0 - 4/t_c\right), \tag{3.5}$$

where, based on Eq. (3.4), we expect t_c to be of the order of $\sqrt{|\gamma_0|t_0}$. Hence Eq. (2.5) becomes

$$\Delta_n = \frac{|\gamma_0|t_0}{4} \sum_{n'=0}^{n_{\max}} \frac{4/t_c - \ln(n+n'+1)}{n'+1/2} \Delta_{n'}. \tag{3.6}$$

Here $n_{\max} = 1/(2\pi T_c\tau) \simeq \exp(4/t_c)$. Again Eq. (3.6) can be considered as the maximal eigenvalue problem for the matrix $M_{nn'}(\zeta) = (\zeta - \ln(n+n'+1))/(n'+1/2)$ with $\zeta = 4/t_c$. Numerical solution for the maximal eigenvalue reveals $\lambda_M \approx$

$0.41(4/t_c)^2$ (see Appendix C). Thus we find

$$t_c \approx 1.3\sqrt{|\gamma_0|t_0}. \tag{3.7}$$

The dependence of the right eigenvector corresponding to the maximal eigenvalue found numerically is shown in Fig. 1.

Similar to the case $\mathcal{N} = 1$, we are able to solve the linearized self-consistency equation (2.5) analytically. Introducing the variable

$$u_\varepsilon = \frac{4}{t(L_\varepsilon)} = \frac{4|\gamma(L_\varepsilon)|}{|\gamma_0|t_0} = \frac{4}{t_0} - \ln(\varepsilon\tau), \tag{3.8}$$

replacing $\ln(n + n' + 1)$ with $\ln(\max\{n + 1/2, n' + 1/2\})$, and using the Euler-Maclaurin formula, we get

$$\frac{4\Delta_{u_n}}{|\gamma_0|t_0} = u_n \int_{u_n}^{u_0} du\Delta_u + \int_{u_\infty}^{u_n} duu\Delta_u + au_n\Delta_{u_0}. \tag{3.9}$$

Here a coincides with the one defined in Eq. (2.9c). Next, writing $\Delta_{u_n} = \Delta_{u_0} f(u_n)$ with $f(u_0) = 1$, we cast the above equation in the following differential equation,

$$\begin{gathered} f''(u) = -(|\gamma_0|t_0/4)f(u), \\ f(u_0) = 1, \quad f'(u_\infty) = \frac{f(u_\infty)}{u_\infty}, \quad f'(u_0) = \frac{|\gamma_0|t_0}{4}. \end{gathered} \tag{3.10}$$

The latter can be elementary solved:

$$f(u) = \frac{F_0(u)}{F_0(u_0)}, \quad F_0(u) \simeq \sin\left[u\sqrt{|\gamma_0|t_0/4}\right] \tag{3.11}$$

Again, in the above equation the solution to $f(u)$ is written in the lowest order in the small parameters $|\gamma_0| \ll t_0 \ll 1$. The last step is to find $u_0 = 4/t_c$ from the relation $f'(u_0) = |\gamma_0|t_0/4$. Simple algebra yields

$$u_0 \simeq \pi/\sqrt{|\gamma_0|t_0}, \quad \Leftrightarrow \quad t_c \simeq \frac{4}{\pi}\sqrt{|\gamma_0|t_0}. \tag{3.12}$$

We point out remarkable agreement between the numerical and the analytical results, Eq. (3.7) and Eq. (3.12): 1.3 and $4/\pi$, respectively.

The numerical solution of Eq. (3.6) for T_c with arbitrary values of t_0 is shown in Fig. 2. Analytical expression (3.12) (marked with a black dotted line) gives correct asymptotic values of $\ln T_c/T_c^{(BCS)}$ in the regime of large ratio $t_0/|\gamma_0|$.

3.2 The Spectral Gap Function

3.2.1 The Gap Function Near T_c

At temperatures $T_c - T \ll T_c$ we use Eq. (2.13) in order to find Δ_ε. We parametrize the temperature T by t_T, such that $T = (2\pi\tau)^{-1}\exp(4/t_0 - 4/t_T)$. After one writes $\Delta_\varepsilon = \Delta_0(T)r_n$, Eq. (2.13) becomes

$$\lambda_M r_n \simeq \sum_{n'=0}^{n_{\max}} M_{nn'}(4/t_T)\left[r_{n'} - \frac{\frac{\Delta_0^2(T)}{8\pi^2 T_c^2} r_{n'}^3}{(n'+1/2)^2}\right], \tag{3.13}$$

Here, we remind, λ_M denotes the maximal eigenvalue of the matrix $M_{nn'}(4/t_c)$. Using the identity $M_{nn'}(4/t_T) = M_{nn'}(4/t_c) + (4/t_T - 4/t_c)/(n'+1/2)$ and approximation $4/t_T - 4/t_c \approx (T_c - T)/T_c$, we rewrite Eq. (3.13) as

$$\lambda_M(4/t_c)r_n \simeq \sum_{n'=0}^{n_{\max}} M_{nn'}(4/t_c)\left[r_{n'} - \frac{\frac{\Delta_0^2(T)}{8\pi^2 T_c^2} r_{n'}^3}{(n'+1/2)^2}\right] + \frac{T_c - T}{T_c}\sum_{n'=0}^{n_{\max}} \frac{r_{n'}}{n'+1/2}.$$

When $T = T_c$ the gap function turns to zero. This implies that r_n are the components of the leading eigenvector of matrix $M_{nn'}(4/t_c)$. Multiplying Eq. (3.2.1) on the left eigenvector of $M_{nn'}(4/t_c)$, $l_n = r_n/(n+1/2)$, we retrieve the result (2.15) with $b_{\mathcal{N}}$ for $\mathcal{N} = 0$ being

$$b_0 = \frac{7\zeta(3)}{\lambda_M}\frac{\left(\sum\limits_{n}^{n_{\max}} r_n/(n+1/2)\right)^2}{\sum\limits_{n=0}^{n_{\max}} r_n^4/(n+1/2)^3}. \tag{3.14}$$

As in the case of $\mathcal{N} = 1$ one can check that within our approximation $b_0 = 1$ as in the BCS theory. The denominator in the right hand side of Eq. (3.14) is treated in the same fashion as in the case of $\mathcal{N} = 1$. While in the numerator we write $r_n = f(u_n)$, where $f(u)$ is given in Eq. (3.11). Using $F_0(u) = \sin(u/\sqrt{\lambda_M})$ and

$u_0 = \sqrt{\lambda_M}\pi/2$, one immediately finds

$$\left(\sum_{n=0}^{n_{\max}} \frac{r_n}{n+1/2}\right)^2 \simeq \left(\int_0^{u_0} du\ f(u)\right)^2 = \lambda_M. \tag{3.15}$$

Therefore, combining the results for numerator and denominator we restore $b_0 = 1$.

3.2.2 The Gap Function at $T \ll T_c$

The spectral gap function at $T = 0$ can be found in the same way as it was done in Sec. 2.2.2 for $\mathcal{N} = 1$. After straightforward calculations, we find

$$\Delta_\varepsilon \simeq \Delta_0 \begin{cases} 1, & \varepsilon \lesssim \Delta_0, \\ F_0(u_\varepsilon)/F_0(u_{\Delta_0}), & \varepsilon \gtrsim \Delta_0. \end{cases} \tag{3.16}$$

The maximal magnitude of the spectral gap, Δ_0, is given by the expression similar to Eq. (3.5),

$$\Delta_0 = (2\pi\tau)^{-1} e^{4/t_0 - 4/t_{\Delta_0}}, \quad t_{\Delta_0} \sim \sqrt{|\gamma_0| t_0}. \tag{3.17}$$

Unfortunately, within our approximation we cannot unambiguously determine the numerical factor in the ratio $t_{\Delta_0}/\sqrt{|\gamma_0|t_0}$ since it requires knowledge of the precise dependence of the infrared lengthscale $L_{E_\varepsilon + E_{\varepsilon'}}$ on Δ_ε and $\Delta_{\varepsilon'}$, see Eq. (1.3). Since t_{Δ_0} stands in the exponent of the expression for Δ_0, we cannot exclude a possibility that Δ_0 differs parametrically from T_c.

We note that the superconducting order parameter (which coincides with the spectral gap function at energies $\varepsilon \sim 1/\tau$) is proportional to $\Delta_0\sqrt{|\gamma_0|/t_0} \ll \Delta_0$. Typical dependence of Δ_ε on ε is shown in Fig. 3.

The change of Δ_ε with increasing temperature is the same as in the case of $\mathcal{N} = 1$. At $T \ll T_c$ the amplitude Δ_0 is decreasing in accordance with Eq. (2.26).

4 Local Density of States

In this section, we discuss the local density of states and its mesoscopic fluctuations in the superconducting state. For the sake of simplicity, we consider $T = 0$.

The disorder-averaged density of states can be found from the solution of the Usadel equation

$$\langle\rho(E)\rangle = \nu\Re\cos\theta_{\varepsilon\to -iE+0} = \nu\Re\frac{\varepsilon}{\sqrt{\varepsilon^2+\Delta_\varepsilon^2}}\Big|_{\varepsilon\to -iE+0}. \tag{4.1}$$

Here the analytical continuation from Matsubara energies to real energies is performed, $i\varepsilon \to E + i0$.

The behavior of the density of states at energies E close to Δ_0 depends on fine structure of Δ_ε at $\varepsilon \sim \Delta_0$. Thus we have no access to these range of energies. The only statement is possible to make is the existence of the spectral gap of the order of Δ_0. Away from Δ_0, i.e. at $E \gtrsim \Delta_0$, using the smallness of $\Delta_\varepsilon/\varepsilon$, we find

$$\frac{\langle\rho(E)\rangle}{\nu} \simeq 1 + \Re\frac{\Delta^2(E)}{2E^2} \simeq 1 + \frac{\Delta_0^2}{2E^2}\frac{F_{\mathcal{N}}^2(u_E)}{F_{\mathcal{N}}^2(u_{\Delta_0})}. \tag{4.2}$$

Here $u_E = u_{\Delta_0}(E/\Delta_0)^{-t_0/2}$ and $u_E = u_{\Delta_0} - \ln(E/\Delta_0)$ for $\mathcal{N} = 1$ and 0, respectivelty.

Now we estimate mesoscopic fluctuations of the local density of states. This can be done using the nonlinear sigma model approach in a way similar to the one of Ref. [37]. We restrict our consideration by energy range

$$\Delta_0 \ll \frac{1}{\tau}e^{-2(2-\mathcal{N})/t_0} \ll E \lesssim \frac{1}{\tau}. \tag{4.3}$$

In this range we can neglect the energy dependence of Δ_ε and approximate it by its non-renormalized value Δ. Then we obtain for the variance of the local density of states the following result (see Appendix D)

$$\frac{\langle[\delta\rho(E,\boldsymbol{r})]^2\rangle}{\nu^2} = \frac{1+\mathcal{N}}{g}\,\mathrm{Re}\int\frac{d^2\boldsymbol{q}}{(2\pi)^2}\left[\frac{2E^2-\Delta^2}{E^2-\Delta^2}\frac{1}{q^2} + \frac{\Delta^2}{E^2-\Delta^2}\frac{D}{Dq^2+2i\sqrt{E^2-\Delta^2}}\right]. \tag{4.4}$$

We note that the contribution in the first line of Eq. (4.4) corresponds to correlations between electron-like and electron-like excitations. They do not feel the

superconducting spectral gap. This explains why the infrared divergence in diffusive propagator persist inside superconductor. The contribution in the second line of Eq. (4.4) is due to correlations between electron-like and hole-like excitations which are split by the twice the superconducting gap.

Performing integration over momentum and expansion in $\Delta/E \ll 1$, we find

$$\frac{\langle[\delta\rho(E,\boldsymbol{r})]^2\rangle}{\langle\rho(E)\rangle^2} = \frac{(1+\mathcal{N})t_0}{2}\Big(\ln\frac{L}{\ell} + \frac{\Delta^2}{2E^2}\ln\frac{L_E}{\ell}\Big). \tag{4.5}$$

We emphasize logarithmic divergence of the variance with the system size L. This signals about strong mesoscopic fluctuations of the local density of states in disordered superconductors with the spin-orbit coupling similar to the case when the spin-orbit coupling is absent [37, 38].

The renormalization of diffusive propagator ignored so far results in substitution of L by $\min\{L, L_E^{(\phi)}\}$ where $L_E^{(\phi)}$ denotes the dephasing length induced by electron-electron interactions. Unfortunately, at present, there is no complete theory of dephasing rate in disordered superconductors. Using the results of Ref. [59], one can estimate dephasing length due to electron-electron interaction at $E \gg \Delta$ as $L_\Delta/(|\gamma_0|\sqrt{t_0}) \gg L_\Delta$. We note that such estimate is applicable at $T \ll T_c$. Close to superconducting transition the dephasing rate is enhanced due to the superconducting fluctuations (for details see Ref. [60]).

With the help of the renormalization group we can convert the perturbative, infrared divergent, result (4.5) into the result for the second moment of the local density of state:

$$\frac{\langle\rho^2(E,\boldsymbol{r})\rangle}{\langle\rho(E)\rangle^2} = \begin{cases} (\min\{L, L_E^{(\phi)}\}/\ell)^{t_0}, & \mathcal{N}=1, \\ 1+(t_0/2)\ln(\min\{L, L_E^{(\phi)}\}/\ell), & \mathcal{N}=0. \end{cases} \tag{4.6}$$

One can also generalize expression (4.5) to the pair correlation function of the local density of states at differing energies $E \gg \Delta$ and $E' = E+\omega \gg \Delta$ (see Appendix D),

$$\frac{\langle\delta\rho(E,\boldsymbol{r})\delta\rho(E',\boldsymbol{r})\rangle}{\langle\rho(E)\rangle\langle\rho(E')\rangle} \simeq \frac{(1+\mathcal{N})t_0}{2}\ln\frac{\min\{L, L_E^{(\phi)}, L_\omega\}}{\ell}. \tag{4.7}$$

For the autocorrelation function of moments one can use Eq. (4.6) in which $\min\{L, L_E^{(\phi)}\}$ should be substituted by $\min\{L, L_E^{(\phi)}, L_\omega\}$.

We note that one can compute the disorder-averaged higher moments of the local density of states. Similarly to the case without spin-orbit interaction [37], the moments correspond to the log-normal distribution for the local density of states.

We would like to acknowledge the recent experimental work [61] that provides valuable insights into the interplay of superconductivity and disorder in two-dimensional systems. Our theoretical study, which investigates strong mesoscopic fluctuations in disordered systems, is in qualitative agreement with their experimental observations. Specifically, our calculations demonstrate similar trends in the emergent strong fluctuations of the local density of states (LDOS) and suggest that fluctuations of spectral gap are rather small, see Eq. (6.1) of Conclusion. It is also important to note that in this work, an epitaxial monolayer of lead is believed to exhibit superconducting behavior in the weak-antilocalization regime, which is directly relevant to the focus of this thesis.

5 Beyond the Lowest Order in Interaction

As noted earlier, the approach presented in this work is limited to the lowest order in disorder and small interaction constants. However, it is of interest to go beyond the framework of lowest order perturbation theory (in small parameters $|\gamma_{s,t,c}| \ll 1$) in order to address a number of important questions. For instance, this would enable us to estimate the interaction-induced inelastic scattering time or verify the assumption that a fully self-consistent expression can be obtained from (1.3) by replacing Δ with Δ_ε in E_ε. The latter would shed light on the puzzle of whether Δ_0 and T_c could be parametrically different, given that they are determined by different limiting equations. Among other factors, the motivation for considering higher orders in $\gamma_{s,t,c}$ is also connected to the interest to understand how the collective modes in a superconductor (see [62] for a detailed review) influence the solutions of the self-consistency equation.

To obtain the one-loop renormalized equations in the higher order in interaction, one needs to account for fluctuations around the saddle point solution. However, in this case, relying solely on the bare expression for the Cooperon is insufficient and the renormalization of the Cooperon due to the interaction must also be taken into account.

Appendix E provides detailed calculations that lead to the following expression for the renormalized Cooperon in the second order of interaction

$$\begin{aligned}\langle \Phi^{\alpha_1\alpha_2,(r,j)}_{\varepsilon_1,-\varepsilon_2,b}(q)\bar\Phi^{\alpha_3\alpha_4,(r,j)}_{-\varepsilon_3,\varepsilon_4,b'}(-q)\rangle &= \langle \Phi^{\alpha_1\alpha_2,(r,j)}_{\varepsilon_1,-\varepsilon_2,b}(q)\Phi^{\alpha_3\alpha_4,(r,j)}_{\varepsilon_4,-\varepsilon_3,b'}(-q)\rangle(\delta_{b'1}m_{rj}+\delta_{b'2}m_{0j}) = \\ &= \frac{2}{g}(\delta_{b,1}m_{rj}+\delta_{b,2}m_{0j})\left[[\hat A_{r,j}(q)]^{-1}\right]^{\alpha_1\alpha_4;\alpha_2\alpha_3}_{\varepsilon_1\varepsilon_4;\varepsilon_2\varepsilon_3;bb'}(\delta_{b',1}m_{rj}+\delta_{b',2}m_{0j}) \qquad (5.1)\end{aligned}$$

where $m_{rj} = (\delta_{r\neq 3}-\delta_{r3})(\delta_{j0}-\delta_{j\neq 0})$ and the Φ-fields are related to the perturbative functions $w^{\alpha\beta}_{n_1n_2} = \sum_{r,j}[w_{rj}(\boldsymbol{p})]^{\alpha\beta}_{n_1n_2}t_{rj}$, see (A.16), via

$$\begin{aligned}\boldsymbol{\Phi}^{\alpha\beta,(0,j)}_{\varepsilon,-\varepsilon'} &= \left([w_{0j}]^{\alpha\beta}_{\varepsilon,-\varepsilon'},[w_{1j}]^{\alpha\beta}_{\varepsilon,-\varepsilon'}\right)^T, \quad \boldsymbol{\Phi}^{\alpha\beta,(3,j)}_{\varepsilon,-\varepsilon'} = \left([w_{3j}]^{\alpha\beta}_{\varepsilon,-\varepsilon'},[w_{2j}]^{\alpha\beta}_{\varepsilon,-\varepsilon'}\right)^T, \\ \bar{\boldsymbol{\Phi}}^{\alpha\beta,(0,j)}_{-\varepsilon',\varepsilon} &= \left([\bar w_{0j}]^{\alpha\beta}_{-\varepsilon',\varepsilon},[\bar w_{1j}]^{\alpha\beta}_{-\varepsilon',\varepsilon}\right)^T, \quad \bar{\boldsymbol{\Phi}}^{\alpha\beta,(3,j)}_{-\varepsilon',\varepsilon} = \left([\bar w_{3j}]^{\alpha\beta}_{-\varepsilon',\varepsilon},[\bar w_{2j}]^{\alpha\beta}_{-\varepsilon',\varepsilon}\right)^T. \qquad (5.2)\end{aligned}$$

The inverse operator $[\hat A_{r,j}(q)]^{-1}$ appearing in (5.1) is essentially the kernel of the

fluctuations action,

$$S_{\text{fl}}^{(2)}[\theta, W] = -\frac{g}{4}\int_q \sum_{\{\varepsilon_i>0\}} \sum_{\substack{r=0,3\\ j=0,1,2,3}} \sum_{bb'=1,2} \sum_{\{\alpha_i\}} \Phi^{\alpha_1\alpha_2,(r,j)}_{\varepsilon_1,-\varepsilon_2,b}(\boldsymbol{q})[\hat{A}_{r,j}(q)]^{\alpha_1\alpha_4;\alpha_2\alpha_3}_{\varepsilon_1\varepsilon_4;\varepsilon_2\varepsilon_3;bb'} (\delta_{b',1}m_{rj} + \delta_{b',2}m_{0j})\Phi^{\alpha_4\alpha_3,(r,j)}_{\varepsilon_4,-\varepsilon_3,b'}(-\boldsymbol{q}). \tag{5.3}$$

It is clear that the resolvent of $\hat{A}_{r,j}(q)$ contains terms that arise due to the accounting of interactions between quasiparticles. In the first order, as $\Gamma_{s,t,c}/Z_\omega \to 0$, one can easily demonstrate that

$$\begin{aligned}[[\hat{A}_{r,j}(q)]^{-1}]^{\alpha_1\alpha_4;\alpha_2\alpha_3}_{\varepsilon_1\varepsilon_4;\varepsilon_2\varepsilon_3;bb'} = \mathcal{D}_q^{(0)}(i\varepsilon_1, i\varepsilon_2)\delta^{\alpha_1\alpha_4}\delta^{\alpha_2\alpha_3}\Bigg\{ &\delta_{\varepsilon_2\varepsilon_3}\delta_{\varepsilon_1\varepsilon_4}\delta_{bb'} \\ &- \frac{16\pi T}{g}\delta^{\alpha_1\alpha_2}\mathcal{D}_q^{(0)}(i\varepsilon_3, i\varepsilon_4)\Bigg[(\delta_{j0}\Gamma_s + \delta_{j\neq 0}\Gamma_t)\hat{X}^{(r,j)}_{bb'}(\varepsilon_1,\varepsilon_2;\varepsilon_3,\varepsilon_4) \\ &+ \delta_{j0}\Gamma_c\left(\hat{Y}^{(r)}_{bb'}(\varepsilon_1,\varepsilon_2;\varepsilon_3,\varepsilon_4) - \frac{(2\pi)^2\delta(\boldsymbol{q})}{V}Y^{(r)}_{0,b}(\varepsilon_1,\varepsilon_2)[Y^{(r)}_{0,b'}(\varepsilon_4,\varepsilon_3)]^*\right)\Bigg]\Bigg\}.\end{aligned} \tag{5.4}$$

As expected, the first line corresponds to the bare value of the correlator, which does not take into account the interaction between quasiparticles. While the expressions in the second and third lines correct this value and make it dependent on the interaction constants. Here, the functions $\hat{X}^{(r,j)}_{bb'}$, $\hat{Y}^{(r)}_{bb'}$, and $Y^{(r)}_{0,b}$ are introduced that depend on the Matsubara energies. The exact expressions for them can be found in the appendix E. We also note that the last term in Eq. (5.4) is negligible due to its small magnitude, which is inversely proportional to the size of the system $(1/V)$.

5.1 The Modified Usadel Equation

Knowing the expression for the renormalized Cooperon (5.1), we can now write down the effective action and derive the renormalized Usadel equation up to second order in the interaction constants. The latter is obtained by varying the effective action with respect to the spectral angle.

After some calculations, details of which can be found in App. F, we get the

following lengthy expressions for the modified gap and Finkel'stein frequency Z_ε

$$\begin{aligned}\Delta_\varepsilon^{(2)} = {}& \frac{2\pi\mathcal{N}T\Gamma_t\gamma_t}{g}\int_q\sum_{\varepsilon'>0}\sin\theta_{\varepsilon'}\mathcal{D}_q^{(0)}(i\varepsilon,i\varepsilon')\left[\Pi^{(t)}(\varepsilon+\varepsilon',q)+\Pi^{(t)}(|\varepsilon'-\varepsilon|,q)\right]\\ & -\frac{2\pi T\Gamma_s\gamma_s}{g}\int_q\sum_{\varepsilon'>0}\sin\theta_{\varepsilon'}\mathcal{D}_q^{(0)}(i\varepsilon,i\varepsilon')\left[\Pi^{(s)}(\varepsilon+\varepsilon',q)+\Pi^{(s)}(|\varepsilon'-\varepsilon|,q)\right]\\ & +\frac{4\pi T\Gamma_c\gamma_c}{g}\int_q\sum_{\varepsilon'>0}\sin\theta_{\varepsilon'}\mathcal{D}_q^{(0)}(i\varepsilon,i\varepsilon')\left[\Pi_\perp^{(c)}(\varepsilon+\varepsilon',q)+\Pi_\perp^{(c)}(|\varepsilon'-\varepsilon|,q)\right]\\ & -\frac{8\pi T\Gamma_c\gamma_s}{g}\int_q\sum_{\varepsilon'>0}\cos\theta_{\varepsilon'}\mathcal{D}_q^{(0)}(i\varepsilon,i\varepsilon')\left[\Pi_A^{(c)}(\varepsilon+\varepsilon',q)+\Pi_A^{(c)}(|\varepsilon'-\varepsilon|,q)\operatorname{sgn}(\varepsilon'-\varepsilon)\right]\end{aligned} \tag{5.5}$$

Here, the superscript «2» indicates that it is an expression for the second order in interaction constants. Preceding orders are not explicitly indicated here and are detailed in Eq. (1.2). The Finskel'stein frequency renormalizes as

$$\begin{aligned}\varepsilon Z_\varepsilon^{(2)} = {}& \frac{2\pi\mathcal{N}T\Gamma_t\gamma_t}{g}\int_q\sum_{\varepsilon'>0}\cos\theta_{\varepsilon'}\mathcal{D}_q^{(0)}(i\varepsilon,i\varepsilon')\left[\Pi^{(t)}(\varepsilon+\varepsilon',q)-\Pi^{(t)}(|\varepsilon'-\varepsilon|,q)\right]\\ & +\frac{2\pi T\Gamma_s\gamma_s}{g}\int_q\sum_{\varepsilon'>0}\cos\theta_{\varepsilon'}\mathcal{D}_q^{(0)}(i\varepsilon,i\varepsilon')\left[\Pi^{(s)}(\varepsilon+\varepsilon',q)-\Pi^{(s)}(|\varepsilon'-\varepsilon|,q)\right]\\ & -\frac{4\pi T\Gamma_c\gamma_c}{g}\int_q\sum_{\varepsilon'>0}\cos\theta_{\varepsilon'}\mathcal{D}_q^{(0)}(i\varepsilon,i\varepsilon')\left[\Pi_\parallel^{(c)}(\varepsilon+\varepsilon',q)-\Pi_\parallel^{(c)}(|\varepsilon'-\varepsilon|,q)\right]\\ & -\frac{8\pi T\Gamma_c\gamma_s}{g}\int_q\sum_{\varepsilon'>0}\sin\theta_{\varepsilon'}\mathcal{D}_q^{(0)}(i\varepsilon,i\varepsilon')\left[\Pi_A^{(c)}(\varepsilon+\varepsilon',q)-\Pi_A^{(c)}(|\varepsilon'-\varepsilon|,q)\operatorname{sgn}(\varepsilon'-\varepsilon)\right]\end{aligned} \tag{5.6}$$

Here we have introduced some convenient notations $\Pi^{(t,s)}(\omega,q)$ and $\Pi^{(c)}_{\perp,\parallel,A}(\omega,q)$, the details of which can be found in Appendix F.

A few remarks are in order here. First, we point out that the new expression for the spectral gap Δ_ε has a much more complex structure in energies ε and ε'. This suggests that while it is tempting to assume that one can simply substitute Δ with Δ_ε in Eq. (1.3), this calculation prohibits this simple trick.

It is also important to note that there was no impact from the renormalization of the Z_ε frequency in the first order. However, as we can clearly see from the

second order, this is no longer the case and can potentially lead to interesting solutions to be obtained in the future. We would like to remind that Z_ε corresponds to the renormalization of some physical parameters, such as heat capacity. We would also like to remind the reader that the formal solution to the homogeneous Usadel equation is actually dependent on the ratio of Δ_ε to Z_ε, rather than on Δ_ε alone. Indeed, it can be written as

$$\sin\theta_\varepsilon = \frac{\Delta_\varepsilon/Z_\varepsilon}{\sqrt{\varepsilon^2 + (\Delta_\varepsilon/Z_\varepsilon)^2}}$$

Finally, we would like to note that our second-order calculation coincides, in the relevant order, with the most general answers obtained independently by P. Nosov, and the author is thankful for sharing his work.

5.2 Limiting Condition: T Near T_c

In the vicinity of the critical temperature, we can linearize the renormalized Usadel equation, bearing in mind that as the temperature approaches T_c, spectral angles θ_ε vanish. This allows us to neglect the superconducting part in diffusons and set $E_\omega = \omega$ everywhere in $\mathcal{D}_q^{(0)}(i\varepsilon, i\varepsilon')$. In what follows, I denote $\bar{\mathcal{D}}_q(i\varepsilon, i\varepsilon')^{-1} = q^2 + (\varepsilon + \varepsilon')/D$.

Knowing the structure of the operators in Eq. (5.5), see Eqs. (F.6) - (F.10), we can readily find

$$\Delta_\varepsilon = 2\pi T \sum_{\varepsilon'>0} \theta_{\varepsilon'} \Bigg(-\gamma_c + 2\frac{(\gamma_s - \mathcal{N}\gamma_t)}{g} \int_q \bar{\mathcal{D}}_q(i\varepsilon, i\varepsilon') - \\ - 4\pi T \frac{\gamma_c(\gamma_s + \mathcal{N}\gamma_t + 2\gamma_c)}{g} \sum_{\varepsilon''>0} \int_q \frac{\bar{\mathcal{D}}_q^2(i\varepsilon, i\varepsilon'')}{D} + 8\pi T \frac{\gamma_s\gamma_c}{g} \sum_{\varepsilon''>0} \int_q \frac{\bar{\mathcal{D}}_q^2(i\varepsilon, i\varepsilon'')}{D} \Bigg), \tag{5.7}$$

where I have kept only the logarithmically divergent terms. Let's discuss each of the contributions briefly. The first line of equation (5.7) consists of two contributions. The first term represents the non-renormalized interaction constant, while the second term corresponds to the renormalization in the lowest order in $\gamma_{s,t,c}$. It's worth noting that this is equivalent to equation (1.2).

The first term in the second line arises from differentiating the Cooperon with

respect to the spectral angle. It corresponds to taking the derivative of the first line of equations (F.2) - (F.4). Finally, the last term arises as a consequence of the mixing of spin-zero modes from the singlet and Cooper channels.

By carefully evaluating the sums and integrals in equation (5.7), we find that in the vicinity of the critical temperature, the expression within the parentheses simplifies to a running interaction constant. This can be compared with Eqs. (18)-(21) in [31],

$$-d\gamma_c = \frac{(\gamma_s - \mathcal{N}\gamma_t)}{\pi g} dy + \frac{\gamma_c(\gamma_s - \mathcal{N}\gamma_t - 2\gamma_c)}{\pi g} dy. \tag{5.8}$$

This suggests that the critical temperature is determined by the behavior of the renormalized interaction constants in the normal state.

6 Conclusion

In summary, we have developed a theory for the multifractally-enhanced superconducting state in thin films with spin-orbit coupling. Our theory is based on the assumption of weak short-ranged electron-electron interaction. We considered two cases: Ising spin-orbit coupling ($\mathcal{N}=1$), where the renormalization of the normal state resistance is negligible, and strong spin-orbit coupling ($\mathcal{N}=0$), where the renormalization of t is dominated by weak-antilocalization correction. In addition to these cases, we also studied the case without spin-orbit coupling ($\mathcal{N}=3$), which was previously discussed in Ref. [37]. With these three cases, we now have a theory that covers all possible behaviors of the normal state resistance with respect to the system size: increasing, decreasing, and constant.

Following the approach of Ref. [37], we considered fluctuations around the mean-field spatially homogeneous saddle-point and derived modified Usadel and self-consistency equations that capture the interplay of disorder and interactions at high energies. These derived equations enable us to accurately determine the superconducting transition temperature. Interestingly, even in the presence of disorder, the transition temperature is enhanced compared to the BCS result in the absence of disorder, including for the case of strong spin-orbit coupling ($\mathcal{N}=0$). Solving the modified Usadel and self-consistency equations yields T_c, which is parametrically consistent with the estimate obtained from the Cooper-channel instability in the renormalization group equations for the normal phase. It is worth comparing the multifractally increased critical temperatures for different numbers of triplet modes. In the absence of spin-orbit coupling, as discussed in Ref. [37], the superconducting phase is expected to exist for temperatures lower than $T_c^{\mathcal{N}=3} \sim \tau^{-1}\exp(-2/t_0)$. In contrast, our predictions for $\mathcal{N}=1$ and $\mathcal{N}=0$ are $T_c^{\mathcal{N}=1} \sim \tau^{-1}\exp(-(2/t_0)\ln(t_0/(1.4|\gamma_0|)))$ and $T_c^{\mathcal{N}=0} \sim \tau^{-1}\exp(-3.1/\sqrt{|\gamma_0|t_0})$, respectively. Therefore, the critical temperature increases with the number of triplet diffusive modes: $T_c^{\mathcal{N}=3} \gg T_c^{\mathcal{N}=1} \gg T_c^{\mathcal{N}=0}$.

The presence of disorder induces an energy dependence in the effective attraction, which in turn affects the energy dependence of the spectral gap function. The specific form of this energy dependence is influenced by the number of triplet modes, denoted as $\mathcal{N}$. In the case of $\mathcal{N}=1$, as well as $\mathcal{N}=3$, the energy dependence of the spectral gap is concave, as depicted in Fig. 3. Conversely, for $\mathcal{N}=0$, the spectral gap function Δ_ε becomes a convex function of ε. The interplay be-

tween disorder and interactions leads to a parametric enhancement of the spectral gap function at low energies compared to its magnitude at energies on the order of $1/\tau$.

In spite of the strong deviation from the BCS theory, where the spectral gap function is energy-independent, the fundamental aspects of the BCS model remain valid for weakly disordered films. This includes the behavior of the gap just below T_c and at low temperatures $T \ll T_c$. Hence, the temperature dependence of the spectral gap in such films can still be described using the BCS theory. In the presence of spin-orbit coupling, we have observed significant mesoscopic fluctuations in the local density of states within the superconducting state. These fluctuations persist up to the length scale determined by the dephasing length. The presence of spin-orbit coupling leads to a reduction in the amplitude of the variance of the local density of states by a factor of 2 (for $\mathcal{N} = 1$) and by a factor of 4 (for $\mathcal{N} = 0$). The energy dependence of the variance is sensitive to the number of massless triplet modes, owing to the different energy dependencies of the gap function for different $\mathcal{N}$ values. The most pronounced differences are expected to occur near the coherence peak at $E \sim \pm\Delta_0$. However, it is important to note that this region falls beyond the accuracy of our calculations.

It is instructive to compare the fluctuations of the local density of states with the fluctuations of the superconducting order parameter. While our approach assumes a spatially constant order parameter, it is still possible to investigate its mesoscopic fluctuations. In the presence of spin-orbit coupling, we have found that

$$\frac{\langle(\delta\Delta)^2\rangle}{\Delta^2} \simeq \frac{(1+\mathcal{N})t_0}{2} \ln\frac{L_{\Delta_0}}{\ell}. \tag{6.1}$$

We would like to emphasize the close similarity between Eqs. (4.7) and (6.1). However, there is a crucial difference: the mesoscopic fluctuations of the superconducting order parameter are governed by the coherence length L_{Δ_0} in the infrared regime. Since $L_E^{(\phi)} \gg L_{\Delta_0}$, we expect $\langle(\delta\rho)^2\rangle/\langle\rho\rangle^2 \gg \langle(\delta\Delta)^2\rangle/\Delta^2$. For $\mathcal{N} = 1$ ($\mathcal{N} = 0$), we can estimate $\langle(\delta\Delta)^2\rangle/\Delta^2$ to be on the order of $\ln(t_0/|\gamma_0|)$ ($\sqrt{t_0/|\gamma_0|}$), respectively.

Also, we have developed a theory that goes beyond the lowest order in interaction. We have demonstrated that in the second order, the structure of the modified Usadel equation becomes more complex, making it no longer amenable to a straightforward replacement of the kernel with an analogous expression from

renormalization group equations in the normal state. However, in the limiting case of temperatures near the critical temperature, the behavior of the spectral gap and T_c is determined by a running constant $\gamma_c(L)$.

The results presented in this thesis can be generalized in several directions. With the developments of P. Nosov for an arbitrary interaction force at our disposal, it becomes intriguing to investigate the influence of collective modes on superconductivity. By employing these new results, one can determine the value of Δ_0 up to a numerical factor, enabling a comparison with the expression for T_c. This ongoing work holds promise for further progress in our understanding of interplay of disorder and superconductivity. On the other hand, our theory can further be extended to include the Coulomb interaction. Additionally, it would be interesting to go beyond weak-coupling for superconductivity and to study multifractal effects at the BCS – BEC crossover [63, 64]. Also our work can be extended to consider systems with singular dynamical interaction between electrons, see Refs. [65, 66, 67, 68, 69, 70], in the presence of disorder. This can be achieved along the approaches of Refs. [71, 72].

Finally, we mention that our theory ignores phase fluctuations of the order parameter. The latter are known to be responsible for the Berezinskii- Kosterlitz-Thouless transition in superconducting films. Such fluctuations can be taken into account in the way similar to the one in Refs. [73, 74]. However, for weakly disordered superconducting films effects related with phase fluctuations are expected to be weak [75, 73].

References

[1] P.W. Anderson, Phys. Rev. 109, 1492 (1958).

[2] D. Belitz and T. R. Kirkpatrick, Rev. Mod. Phys. 66, 261 (1994).

[3] A. Layzer and D. Fay, Int. J. Magn. 1, 135 (1971).

[4] A. Kreisel, Y. Quan, and P. J. Hirschfeld, Phys. Rev. B 105, 104507 (2022).

[5] M. Sato and Y. Ando, Rep. Prog. Phys. 80, 076501 (2017).

[6] S. Hikami, A. I. Larkin, Y. Nagaoka . Prog. Theor. Phys. 63, 707–710 (1980).

[7] N. F. Q. Yuan, B. T. Zhou, W.-Y. He and K. T. Law, AAPPS Bull. 26, 12-9 (2016).

[8] M.I. D'yakonov and V.I. Perel', Sov. Phys. JETP 33, 1053 (1971).

[9] L. P. Gor'kov and E. I. Rashba, Phys. Rev. Lett. 87, 037004 (2001).

[10] A. A. Abrikosov and L. P. Gor'kov, Sov. Phys. JETP 8, 1090 (1959).

[11] A. A. Abrikosov and L. P. Gor'kov, Sov. Phys. JETP 9, 220 (1959).

[12] P. W. Anderson, J. Phys. Chem. Solids 11, 26 (1959).

[13] L. N. Bulaevskii and M. V. Sadovskii, JETP Lett. 39, 640 (1984).

[14] M. Ma and P. A. Lee, Phys. Rev. B 32, 5658 (1985).

[15] A. Kapitulnik and G. Kotliar, Phys. Rev. Lett. 54, 473 (1985).

[16] G. Kotliar and A. Kapitulnik, Phys. Rev. B 33, 3146 (1986).

[17] S. Maekawa and H. Fukuyama, J. Phys. Soc. Jpn. 51, 1380 (1982).

[18] H. Takagi and Y. Kuroda, Solid State Comm. 41, 643 (1982).

[19] S. Maekawa, H. Ebisawa, and H. Fukuyama, J. Phys. Soc. Jpn. 53, 2681 (1984).

[20] P. W. Anderson, K. A. Muttalib, and T. V. Ramakrishnan, Phys. Rev. B 28, 117 (1983).

[21] L. N. Bulaevskii and M. V. Sadovskii, J. Low Temp. Phys. 59, 89 (1985).

[22] A. M. Finkel'stein, JETP Lett. 45, 46 (1987).

[23] A. M. Finkel'stein, Physica B 197, 636 (1994).

[24] D. B. Haviland, Y. Liu, and A. M. Goldman, Phys. Rev. Lett. 62, 2180 (1989).

[25] A. M. Goldman and N. Marković, Phys. Today 51, 39 (1998).

[26] V. F. Gantmakher and V. T. Dolgopolov, Physics-Uspekhi 53, 1 (2010).

[27] B. Sacépé, M. Feigel'man, T. M. Klapwijk, Nat. Phys. 16, 734 (2020).

[28] M. V. Feigel'man, L. B. Ioffe, V. E. Kravtsov, and E. A. Yuzbashyan, Phys. Rev. Lett. 98, 027001 (2007).

[29] M. V. Feigel'man, L. B. Ioffe, V. E. Kravtsov, and E. Cuevas, Ann. Phys. 325, 1390 (2010).

[30] I. S. Burmistrov, I. V. Gornyi, A. D. Mirlin, Phys. Rev. Lett. 108, 017002 (2012).

[31] I. S. Burmistrov, I. V. Gornyi, and A. D. Mirlin, Phys. Rev. B 92, 014506 (2015).

[32] M. N. Gastiasoro and B. M. Andersen, Phys. Rev. B 98, 184510 (2018).

[33] B. Fan and A. M. García-García, Phys. Rev. B 101, 104509 (2020).

[34] M. Stosiek, B. Lang, and F. Evers, Phys. Rev. B 101, 144503 (2020).

[35] K. Zhao, H. Lin, X. Xiao, W. Huang, W. Yao, M. Yan, Y. Xing, Q. Zhang, Z.-X. Li, S. Hoshino, J. Wang, S. Zhou, L. Gu, M. S. Bahramy, H. Yao, N. Nagaosa, Q.-K. Xue, K. T. Law, X. Chen, and S.-H. Ji, Nat. Phys. 15, 904 (2019).

[36] C. Rubio-Verdú, A. M. García-García, H. Ryu, D.-J. Choi, J. Zaldívar, S. Tang, B. Fan, Z.-X. Shen, S.-K. Mo, J. I. Pascual, and M. M. Ugeda, Nano Lett. 20, 5111 (2020).

[37] I. S. Burmistrov, I. V. Gornyi, and A. D. Mirlin, Ann. Phys. (N.Y.) 435, 168499 (2021).

[38] M. Stosiek, F. Evers, and I. S. Burmistrov, Phys. Rev. Research 3, L042016 (2021).

[39] B. Sacépé, C. Chapelier, T. I. Baturina, V. M. Vinokur, M. R. Baklanov, and M. Sanquer, Phys. Rev. Lett. 101, 157006 (2008).

[40] B. Sacépé, C. Chapelier, T. I. Baturina, V. M. Vinokur, M. R. Baklanov, and M. Sanquer, Nat. Commun. 1, 140 (2010).

[41] B. Sacépé, Th. Dubouchet, C. Chapelier, M. Sanquer, M. Ovadia, D. Shahar, M. Feigel'man, and L. Ioffe, Nat. Phys. 7, 239 (2011).

[42] D. Sherman, B. Gorshunov, S. Poran, N. Trivedi, E. Farber, M. Dressel, and A. Frydman, Phys. Rev. B 89, 035149 (2014).

[43] M. Mondal, A. Kamlapure, M. Chand, G. Saraswat, S. Kumar, J. Jesudasan, L. Benfatto, V. Tripathi, and P. Raychaudhuri, Phys. Rev. Lett. 106, 047001 (2011).

[44] Y. Noat, V. Cherkez, C. Brun, T. Cren, C. Carbillet, F. Debontridder, K. Ilin, M. Siegel, A. Semenov, H.-W. Hübers, and D. Roditchev, Phys. Rev. B 88, 014503 (2013).

[45] I. S. Burmistrov, I. V. Gornyi, and A. D. Mirlin, Phys. Rev. B 93, 205432 (2016).

[46] C. Brun, T. Cren, V. Cherkez, F. Debontridder, S. Pons, L. B Ioffe, B. L. Altshuler, D. Fokin, M. C. Tringides, S. Bozhko, and D. Roditchev, Nat. Phys. bf 10, 444 (2014).

[47] M. Kim, Y. Kozuka, C. Bell, Y. Hikita, and H. Y. Hwang, Phys. Rev. B 86, 085121 (2012).

[48] K. Ueno, T. Nojima, S. Yonezawa, M. Kawasaki, Y. Iwasa, and Y. Maeno, Phys. Rev. B 89, 020508(R) (2014).

[49] A. D. Caviglia, S. Gariglio, N. Reyren, D. Jaccard, T. Schneider, M. Gabay, S. Thiel, G. Hammerl, J. Mannhart, and J.-M. Triscone, Nature 456, 624 (2008).

[50] J. A. Sulpizio, S. Ilani, P. Irvin, and J. Levy, Annu. Rev. Mater. Res. 44, 117 (2014).

[51] J. T. Ye, Y. J. Zhang, R. Akashi, M. S. Bahramy, R. Arita, and Y. Iwasa, Science 338, 1193 (2012).

[52] J. T. Ye, Y. J. Zhang, M. Yoshida, Y. Saito, and Y. Iwasa, J. Supercond. Nov. Magn. 27, 981 (2014).

[53] K. Taniguchi, A. Matsumoto, H. Shimotani, and H. Takagi, Appl. Phys. Lett. 101, 042603 (2012).

[54] E.S. Andriyakhina, I.S. Burmistrov, ZhETF 162, 522 (2022).

[55] K. D. Usadel, Phys. Rev. Lett. 25, 507 (1970).

[56] M. A. Skvortsov and M. V. Feigel'man, Phys. Rev. Lett. 95, 057002 (2005).

[57] M. V. Feigel'man and M. A. Skvortsov, Phys. Rev. Lett. 109, 147002 (2012).

[58] P. A. Lee, J. Non-Cryst. Solids, bf 35, 21 (1980).

[59] T. P. Devereaux and D. Belitz, Phys. Rev. B 44, 4587 (1991)

[60] W. Brenig, M.-Ch. Chang, E. Abrahams, and P. Wölfle Phys. Rev. B 31, 7001 (1985).

[61] M. Lizée, M. Stosiek, I. Burmistrov, T. Cren, and C. Brun, Phys. Rev. B 107, 174508 (2023).

[62] I. O. Kulik, Ora Entin-Wohlman, R. Orbach, J. Low Temp. Phys. 43, 591–620 (1981).

[63] Y. L. Loh, M. Randeria, N. Trivedi, Ch.-Ch. Chang, and R. Scalettar, Phys. Rev. X 6, 021029 (2016).

[64] M. Yu. Kagan, E. A. Mazur, JETP 159, 696 (2021).

[65] A. Abanov, A. V. Chubukov, Phys. Rev. B 102, 024524 (2020).

[66] Y. Wu, A. Abanov, Y. Wang, A. V. Chubukov, Phys. Rev. B 102, 024525 (2020).

[67] Y.-M. Wu, A. Abanov, A. V. Chubukov, Phys. Rev. B 102, 094516 (2020).

[68] Y.-M. Wu, Sh.-Sh. Zhang, A. Abanov, A. V. Chubukov, Phys. Rev. B 103, 024522 (2021).

[69] Y.-M. Wu, Sh.-Sh. Zhang, A. Abanov, A. V. Chubukov, Phys. Rev. B 103, 184508 (2021).

[70] Y.-M. Wu, Sh.-Sh. Zhang, A. Abanov, A. V. Chubukov, Phys. Rev. B 104, 144509 (2021).

[71] P. A. Nosov, I. S. Burmistrov, and S. Raghu, Phys. Rev. Lett. 125, 256604 (2020).

[72] T. Ch. Wu, Y. Liao, M. S. Foster, arXiv:2206.01762.

[73] E. J. König, A. Levchenko, I. V. Protopopov, I. V. Gornyi, I. S. Burmistrov, and A. D. Mirlin, Phys. Rev. B 92, 214503 (2015).

[74] E. J. König, I. V. Protopopov, A. Levchenko, I. V. Gornyi, and A. D. Mirlin, Phys. Rev. B 104, 100507 (2021).

[75] M. R. Beasley, J. E. Mooij, and T. P. Orlando, Phys. Rev. Lett. 42, 1165 (1979).

[76] I. S. Burmistrov, I. V. Gornyi, and A. D. Mirlin, Phys. Rev. Lett. 111, 066601 (2013).

[77] I. S. Burmistrov, I. V. Gornyi, and A. D. Mirlin, Phys. Rev. B 91, 085427 (2015).

[78] A. M. Finkel'stein, Electron Liquid in Disordered Conductors, vol. 14 of Soviet Scientific Reviews, ed. by I.M. Khalatnikov, Harwood Academic Publishers, London, (1990).

[79] I. S. Burmistrov, JETP, 129, 669 (2019).

[80] K. B. Efetov, A. I. Larkin, and D. E. Khmel'nitskii, Sov. Phys. JETP 52, 568 (1980).

Appendices

A Details of the Finkel'stein Nonlinear Sigma Model Formalism

In this Appendix we present details of the Finkel'stein nonlinear sigma model formalism.

The action of an electron liquid in a disordered metal with spin-orbit coupling is given by

$$S = S_\sigma + S_{\rm int}^{(\rho)} + S_{\rm int}^{(\sigma)} + S_{\rm int}^{(c)} + S_{\rm so}, \tag{A.1}$$

where the first term comes from non-interacting fermions. The next three terms correspond to electron-electron interactions in the particle-hole singlet channel, $S_{\rm int}^{(\rho)}$, in the particle-hole triplet channel, $S_{\rm int}^{(\sigma)}$, and in the particle-particle channel $S_{\rm int}^{(c)}$. The last term appears due to spin-orbit coupling. The above mentioned contributions reads (see Refs. [78, 2, 79] for review)

$$S_\sigma = -\frac{g}{32}\int_{\boldsymbol{r}} \mathrm{Tr}(\nabla Q)^2 + 2Z_\omega \int_{\boldsymbol{r}} \mathrm{Tr}\,\hat{\varepsilon} Q \tag{A.2a}$$

$$S_{\rm int}^{(\rho)} = -\frac{\pi T}{4}\Gamma_s \sum_{r=0,3}\sum_{\alpha,n}\int_{\boldsymbol{r}} \mathrm{Tr}\, I_n^\alpha t_{r0} Q\, \mathrm{Tr}\, I_{-n}^\alpha t_{r0} Q \tag{A.2b}$$

$$S_{\rm int}^{(\sigma)} = -\frac{\pi T}{4}\Gamma_t \sum_{\substack{r=0,3\\ j=1,2,3}}\sum_{\alpha,n}\int_{\boldsymbol{r}} \mathrm{Tr}\, I_n^\alpha t_{rj} Q\, \mathrm{Tr}\, I_{-n}^\alpha t_{rj} Q \tag{A.2c}$$

$$S_{\rm int}^{(c)} = -\frac{\pi T}{4}\Gamma_c \sum_{r=1,2}\sum_{\alpha,n}\int_{\boldsymbol{r}} \mathrm{Tr}\, t_{r0} L_n^\alpha Q\, \mathrm{Tr}\, t_{r0} L_n^\alpha Q \tag{A.2d}$$

$$S_{\rm so} = \frac{\pi\nu}{2}\sum_{j=1,2,3}\frac{1}{\tau_{\rm so}^{(j)}}\int_{\boldsymbol{r}} \mathrm{Tr}(t_{0j} Q)^2 \tag{A.2e}$$

In what is written above g is the total Drude conductivity (in units e^2/h and including spin). The parameter Z_ω describes the renormalization of the frequency term [78]. Its bare value is given as $\pi\nu/4$. Interaction amplitudes in the singlet, the triplet, and the particle-particle channels are designated as Γ_s, Γ_t, and Γ_c, respectively. It is convenient to introduce the dimensionless interaction parameters $\gamma_{s,t,c} \equiv \Gamma_{s,t,c}/Z_\omega$. $1/\tau_{\rm so}^{(j)}$ stands for the spin-orbit scattering rate in the channel j.

The matrix field $Q(\boldsymbol{r})$ and the trace Tr operate in the replica (α, β), Matsubara (n, m), spin $(j = 0, 1, 2, 3)$, and particle-hole $(r = 0, 1, 2, 3)$ spaces. The matrix field $Q(\boldsymbol{r})$ obeys the nonlinear constraint, as well as the charge-conjugation symmetry relation

$$Q^2 = 1, \quad \mathrm{Tr}\, Q = 0, \quad Q = Q^\dagger = -CQ^T C, \tag{A.3}$$

where $C = it_{12}$ and the matrix t_{rj} is

$$t_{rj} = \tau_r \otimes s_j, \quad r, j = 0, 1, 2, 3. \tag{A.4}$$

In the expression above r and j subscripts correspond to particle-hole and spin spaces, respectively. τ_r and s_j denote standard Pauli matrices,

$$\begin{aligned} \tau_0/s_0 &= \begin{pmatrix} 1 & 0 \\ 0 & 1 \end{pmatrix}, \quad \tau_1/s_1 = \begin{pmatrix} 0 & 1 \\ 1 & 0 \end{pmatrix}, \\ \tau_2/s_2 &= \begin{pmatrix} 0 & -i \\ i & 0 \end{pmatrix}, \quad \tau_3/s_3 = \begin{pmatrix} 1 & 0 \\ 0 & -1 \end{pmatrix}. \end{aligned} \tag{A.5}$$

Taking constraints (A.3) into account, we use the following parametrization for the matrix field $Q(\boldsymbol{r})$

$$\begin{aligned} Q = U^{-1}\Lambda U, \quad U^\dagger = U^{-1}, \quad CU^T = U^{-1}C, \\ \Lambda^{\alpha\beta}_{nm} = \mathrm{sgn}\, \varepsilon_n \delta_{\varepsilon_n, \varepsilon_m} \delta^{\alpha\beta} t_{00} \end{aligned} \tag{A.6}$$

The constant matrices in the action (A.1) are given by the following expressions $(\omega_k = 2\pi T k)$:

$$\begin{aligned} \hat{\varepsilon}^{\alpha\beta}_{nm} &= \varepsilon_n \delta_{\varepsilon_n, \varepsilon_m} \delta^{\alpha\beta} t_{00}, \\ (I^\gamma_k)^{\alpha\beta}_{nm} &= \delta_{\varepsilon_n - \varepsilon_m, \omega_k} \delta^{\alpha\beta} \delta^{\alpha\gamma} t_{00}, \\ (L^\gamma_k)^{\alpha\beta}_{nm} &= \delta_{\varepsilon_n + \varepsilon_m, \omega_k} \delta^{\alpha\beta} \delta^{\alpha\gamma} t_{00}. \end{aligned} \tag{A.7}$$

Following Ref. [37], we employ the above technique to describe the low-energy physics in the broken symmetry superconducting state. In order to do so one needs to single out the static term with $n = 0$ in the particle-particle channel, see Eq. (A.2d), and introduce two decoupling fields $\Delta^\alpha_r(\boldsymbol{r})$ with $r = 1, 2$. Upon

Hubbard–Stratonovich transformation one finds

$$S_{\rm int}^{(c)} = \sum_{r=1,2} \int_{\boldsymbol{r}} \left[\frac{4Z_\omega}{\pi T \gamma_c} [\Delta_r^\alpha(\boldsymbol{r})]^2 + 2Z_\omega \Delta_r^\alpha(\boldsymbol{r}) \,\mathrm{Tr}\, t_{r0} L_0^\alpha Q - \frac{\pi T}{4} \Gamma_c \sum_{n\neq 0} (\mathrm{Tr}\, t_{r0} L_n^\alpha Q)^2 \right]. \tag{A.8}$$

Variation of the total action with respect to $Q(\boldsymbol{r})$ and $\Delta_r^\alpha(\boldsymbol{r})$ give rise to the Usadel equation and the self-consistency relations for $\Delta_r^\alpha(\boldsymbol{r})$, $r = 1, 2$. In turn, these equations may generate many spatially dependent solutions. In order to account for them we assume $1/g \ll 1$ and exploit the renormalization group technique by treating the spatially dependent solutions $Q(\boldsymbol{r})$ as fluctuations around some spatially independent solution $\underline{Q}$.

This program can be performed as follows. At first, we distinguish spatially independent and spatially dependent components of the fields $\Delta_r^\alpha(\boldsymbol{r})$, $r = 1, 2$, they read

$$\Delta_r^\alpha(\boldsymbol{r}) = \underline{\Delta}_r^\alpha + \delta\Delta_r^\alpha(\boldsymbol{r}), \quad \int_{\boldsymbol{r}} \delta\Delta_r^\alpha(\boldsymbol{r}) = 0. \tag{A.9}$$

We point out that fluctuations of the order parameter are now contained in $\delta\Delta_r^\alpha(\boldsymbol{r})$. On the other hand, one can perform a formally exact integration over the fields $\delta\Delta_r^\alpha(\boldsymbol{r})$ in the action. The latter transfers information about fluctuations of the order parameter entirely onto the field $Q(\boldsymbol{r})$. Accordingly, we get

$$S_{\rm int}^{(c)} = 2Z_\omega V \sum_\alpha \sum_{r=1,2} \left\{ \underline{\Delta}_r^\alpha \,\mathrm{Tr}\, t_{r0} L_0^\alpha \overline{Q} + \frac{2}{\pi T \gamma_c} \left[\underline{\Delta}_r^\alpha\right]^2 \right\} + \hat{S}_{\rm int}^{(c)}, \tag{A.10}$$

where V is the volume of a superconductor,

$$\overline{Q} = \frac{1}{V} \int_{\boldsymbol{r}} Q(\boldsymbol{r}), \tag{A.11}$$

and

$$\hat{S}_{\rm int}^{(c)} = -\frac{\pi T}{4} \Gamma_c \sum_{\alpha,n} \sum_{r=1,2} \int_{\boldsymbol{r}} \left(\mathrm{Tr}\, t_{r0} L_n^\alpha Q_n\right)^2 . \tag{A.12}$$

Where $Q_n = Q - \overline{Q}\delta_{n,0}$.

The described above procedure leads to a new saddle-point equation for $Q(\boldsymbol{r})$

and self-consistency equations for $\underline{\Delta}_r^\alpha$,

$$D\nabla(Q\nabla Q) - [\hat{\varepsilon} + \hat{\underline{\Delta}}, Q] + \frac{\pi T}{4}\sum_{\alpha,n}\Bigg[\sum_{r=1,2}\gamma_c[t_{r0}L_n^\alpha, Q]$$
$$\times \operatorname{Tr} t_{r0}L_n^\alpha Q_n + \sum_{r=0,3}\sum_{j=0}^{3}\gamma_j[I_{-n}^\alpha t_{rj}, Q]\operatorname{Tr} I_n^\alpha t_{rj}Q\Bigg] = 0,$$
$$\underline{\Delta}_r^\alpha = \frac{\pi T}{4}|\gamma_c|\operatorname{Tr} t_{r0}L_0^\alpha\overline{Q}, \quad r = 1,2\ . \tag{A.13}$$

Now, one can investigate solutions of the latter equations. In the mean-field description one ignores fluctuations, seeking a spatially independent solution solely. This solution can be conveniently parametrized with the so-called spectral angle, θ_{ε_n}, which is function of Matsubara energies ε_n. In terms of the spectral angle the saddle-point solution reads

$$\underline{Q} = R^{-1}\Lambda R, \qquad R_{nm}^{\alpha\beta} = \left[\delta_{\varepsilon_n,\varepsilon_m}\cos\frac{\theta_{\varepsilon_n}}{2}, -t_\phi\delta_{\varepsilon_n,-\varepsilon_m}\operatorname{sgn}\varepsilon_m\sin\frac{\theta_{\varepsilon_n}}{2}\right]\delta^{\alpha\beta}$$
$$t_\phi = \cos\phi\ t_{10} + \sin\phi\ t_{20}, \qquad \underline{\Delta}_1^\alpha = \Delta\cos\phi, \qquad \underline{\Delta}_2^\alpha = \Delta\sin\phi. \tag{A.14}$$

Substituting the expressions for $\underline{Q}$ and $\underline{\Delta}_r^\alpha$ from (A.14) into the Usadel and self-consistent equations, we find

$$\frac{D}{2}\nabla^2\theta_{\varepsilon_n} - |\varepsilon_n|\sin\theta_{\varepsilon_n} + \Delta\cos\theta_{\varepsilon_n} = 0, \tag{A.15a}$$
$$\Delta = \pi T|\gamma_c|\sum_{\varepsilon_n}\sin\theta_{\varepsilon_n}. \tag{A.15b}$$

The spatially independent solution of Eq. (A.15a) reduces Eq. (A.15b) to the usual self-consistent equation of the BCS theory. Thus T_c becomes insensitive to disorder in accordance with the "Anderson theorem".

However, we are interested in more intricate picture, when fluctuations of $Q(\boldsymbol{r})$ around the saddle-point solution $\underline{Q}$ are taken into consideration. The latter corresponds to the interaction of the diffusive modes. We use the square-root parametrization of the matrix field to get the perturbative expansion of $Q(\boldsymbol{r})$ field around the saddle-point solution,

$$Q = R^{-1}\left(W + \Lambda\sqrt{1 - W^2}\right)R, \quad W = \begin{pmatrix} 0 & w \\ \overline{w} & 0 \end{pmatrix}. \tag{A.16}$$

Here W-field satisfies the charge-conjugation constraints:

$$\overline{w} = -Cw^T C, \qquad w = -Cw^* C. \tag{A.17}$$

Before delving into fluctuations, it is necessary to determine the propagators for the diffusive modes. In this analysis, we consider the lowest order in residual electron-electron interactions, corresponding to small values of the bare interaction parameters $|\gamma_{s0,t0,c0}| \ll 1$. Within this approximation, we obtain

$$\left\langle [w_{rj}(\boldsymbol{p})]^{\alpha_1\beta_1}_{n_1n_2} [\overline{w}_{rj}(-\boldsymbol{p})]^{\beta_2\alpha_2}_{n_4n_3} \right\rangle = \frac{2}{g}\delta^{\alpha_1\alpha_2}\delta^{\beta_1\beta_2}\delta_{\varepsilon_{n_1},\varepsilon_{n_3}}\delta_{\varepsilon_{n_2},\varepsilon_{n_4}}\mathcal{D}^{(0)}_p(i\varepsilon_{n_1}, i\varepsilon_{n_2}),$$
$$\mathcal{D}^{(0)}_p(i\varepsilon_{n_1}, i\varepsilon_{n_2}) = \frac{1}{p^2 + E_{\varepsilon_{n_1}}/D + E_{\varepsilon_{n_2}}/D}. \tag{A.18}$$

Here, we would like to remind that $E_{\varepsilon_n} = |\varepsilon_n|\cos\theta_{\varepsilon_n} + \Delta \sin\theta_{\varepsilon_n}$. It is crucial to keep in mind that the result in Eq. (A.18) disregards the spin-orbit term in the action, $S_{\rm so}$. This omission results in the appearance of an additional mass term (proportional to $1/\tau^{\rm eff}_{\rm so}$, which is a combination of $1/\tau^{(x)}_{\rm so}$, $1/\tau^{(y)}_{\rm so}$, and $1/\tau^{(z)}_{\rm so}$) in the denominator of the diffusive propagators in Equation (A.18). As a consequence, these propagators will be suppressed in the diffusive limit. In other words, the index j in the above equations exclusively accounts for the gapless modes. For $\mathcal{N} = 0$, $j = 0$, and for $\mathcal{N} = 1$, $j = 0, 3$. The precise expression for the correlators, incorporating the spin scattering times $\tau^{(x,y,z)}_{\rm so}$ on the right-hand side, can be found, for instance, in the referenced work [80].

Hereby, we are ready to examine how the fluctuations of Q renormalize the action of the NLSM. To the lowest order in disorder, we approximate Q as $Q \simeq \underline{Q} + R^{-1}WR$. Taking this approximation into account, we obtain the following correction to the action arising from the interaction part (in the particle-hole channel):

$$S^{(\rho)}_{\rm int} + S^{(\sigma)}_{\rm int} \to -\frac{\pi T}{4}\int_{\boldsymbol{r}} \sum_{\alpha,n}\sum_{r=0,3}\sum_{j} \Gamma_j \langle {\rm Tr}\left[RI^{\alpha}_{n} t_{rj} R^{-1} W\right] {\rm Tr}\left[RI^{\alpha}_{-n} t_{rj} R^{-1} W\right]\rangle. \tag{A.19}$$

Here and in subsequent calculations, we perform summation over $j = 0$ for $\mathcal{N} = 0$ and over $j = 0, 3$ for $\mathcal{N} = 1$. Using the expression for the propagators (A.18), we can evaluate the following expressions (for a more detailed derivation,

refer to Ref. [37]):

$$S_{\rm int}^{(\rho)}+S_{\rm int}^{(\sigma)}\to\frac{32\pi TN_rV}{g}(\Gamma_s-\mathcal{N}\Gamma_t)\sum_{\varepsilon,\varepsilon'>0}\sin\theta_\varepsilon\sin\theta_{\varepsilon'}\int_q\mathcal{D}_q^{(0)}(i\varepsilon,-i\varepsilon')\ , \tag{A.20}$$

where $\int_q\equiv\int d^2\boldsymbol{q}/(2\pi)^2$. In turn, the interaction in the Cooper channel undergoes renormalization as follows:

$$\hat{S}_{\rm int}^{(c)}\to-\frac{32\pi T\Gamma_cN_r}{g}\sum_{\varepsilon>0}\mathcal{D}_{q=0}^{(0)}(i\varepsilon,-i\varepsilon)\sin^2\theta_\varepsilon. \tag{A.21}$$

Together Eqs. (A.20) and (A.21) contribute to the following modified action

$$\begin{aligned}S[\underline{Q}]\to 16\pi TZ_\omega N_rV\Bigg\{&\frac{\Delta^2}{4\pi T\gamma_c}+\sum_{\varepsilon>0}\Big[\varepsilon\cos\theta_\varepsilon+\Delta\sin\theta_\varepsilon\Big]\\&+\frac{2\pi T(\gamma_s-\mathcal{N}\gamma_t)}{g}\sum_{\varepsilon,\varepsilon'>0}\sin\theta_\varepsilon\sin\theta_{\varepsilon'}\int_q\mathcal{D}_q^{(0)}(i\varepsilon,-i\varepsilon')\Bigg\}\ .\end{aligned} \tag{A.22}$$

Finally, variation of Eq. (A.22) with respect to θ_ε and Δ, leads to Eqs. (1.1) and (1.2), accordingly.

B The Critical Temperature: Renormalization Group Approach

In this appendix, we employ the renormalization group equations to estimate the critical temperature by considering the renormalization of resistivity and interactions in the normal phase. The complete set of one-loop (lowest order in disorder) renormalization group equations has been derived using the background field renormalization of the Finkel'stein nonlinear sigma model. The corresponding equations can be found in Eqs. (47)-(51) of Ref. [31]. By expanding these

equations in the regime of $|\gamma_{s,t,c}| \ll 1$ and selecting $\mathcal{N} = 1$, we obtain

$$\frac{dt}{dy} = -t^2(\gamma_s + \gamma_t + 2\gamma_c])/2, \tag{B.1a}$$

$$\frac{d}{dy}\begin{pmatrix}\gamma_s\\ \gamma_t\\ \gamma_c\end{pmatrix} = -\frac{t}{2}\begin{pmatrix}1 & 1 & 2\\ 1 & 1 & -2\\ 1 & -1 & 0\end{pmatrix}\begin{pmatrix}\gamma_s\\ \gamma_t\\ \gamma_c\end{pmatrix} - \begin{pmatrix}0\\ 0\\ 2\gamma_c^2\end{pmatrix}. \tag{B.1b}$$

Eq. (B.1a) implies that dimensionless resistance t remains constant and equals to its bare value t_0. Projecting Eqs. (B.1b) onto the BCS line $-\gamma_s = \gamma_t = \gamma_c = \gamma$ we obtain

$$\frac{d\gamma}{dy} = t_0\gamma - \gamma^2, \quad \gamma_0 = (\gamma_{t0} - \gamma_{s0} + 2\gamma_{c0})/4 < 0. \tag{B.2}$$

Upon solving the above equation, we observe that the renormalization group flow diverges at $y_c = t_0^{-1}\ln(1 + t_0/|\gamma_0|)$. In the regime where $|\gamma_0| \ll t_0 \ll 1$, this divergence leads to a significant enhancement of superconductivity, with $T_c \sim (1/\tau)e^{-2y_c}$, as shown in Eq. (2.4). It is worth noting that for $|\gamma_0| \ll t_0 \ll 1$, the attractive interaction γ reaches the value of t_0 at the length-scale $y_c - \ln 2$, after which it rapidly diverges.

Next, we address the case of $\mathcal{N} = 0$ using the same approach. Strong spin-orbit coupling completely suppresses all triplet modes, and the equations for the remaining interactions γ_s, γ_c, and the resistivity t are given by:

$$\frac{dt}{dy} = -t^2/2, \tag{B.3a}$$

$$\frac{d}{dy}\begin{pmatrix}\gamma_s\\ \gamma_c\end{pmatrix} = -\frac{t}{2}\begin{pmatrix}1 & 2\\ 1 & 0\end{pmatrix}\begin{pmatrix}\gamma_s\\ \gamma_c\end{pmatrix} - \begin{pmatrix}0\\ 2\gamma_c^2\end{pmatrix}. \tag{B.3b}$$

Projection of the latter system onto the BCS line $-\gamma_s = \gamma_c = \gamma$ gives

$$\frac{d\gamma}{dy} = (t/2)\gamma - (4/3)\gamma^2, \quad \gamma_0 = (2\gamma_{c0} - \gamma_{s0})/3 < 0. \tag{B.4}$$

Similarly to the case discussed above, in the regime $|\gamma_0| \ll t_0 \ll 1$ $|\gamma|$ grows with increase of y and reaches t. After this happen, $|\gamma|$ very quickly diverges at the length-scale $y_c \sim 1/\sqrt{|\gamma_0|t_0}$. The latter corresponds to the following critical temperature $T_c \sim (1/\tau)e^{-2y_c}$, cf. Eq. (3.4) .

C The Critical Temperature: Exact Numerical Diagonalization

In this appendix, we provide additional details regarding the numerical solution for the critical temperature. To accomplish this, we utilize techniques such as power iteration and dimensional fitting.

As mentioned in the main text, the linearized self-consistency equation in Eq. (2.5) can be viewed as an eigenvalue problem. However, from a numerical standpoint, the challenge arises due to the fact that the matrices defined in Eqs. (2.6) and (3.6) are significantly large in size. In fact, $n_{\max} \simeq 1/2\pi\tau T_c$ leads to $n_{\max} \propto (t_0/|\gamma_0|)^{2/t_0} \gg 1$ for $\mathcal{N} = 1$ and $n_{\max} \propto \exp(4/t_c - 4/t_0) \gg 1$ for $\mathcal{N} = 0$. In the following, we address each case separately.

When considering Ising spin-orbit coupling, we fit the leading eigenvector using the following expression:

$$\lambda_M = c_1/t_0 + c_2, \tag{C.1}$$

where c_1 and c_2 are the fitting parameters. This formula is justified by the following analytical estimate,

$$\lambda_M = \sum_{n'\geqslant 0}^{n_{\max}} \frac{\Delta_{n'}/\Delta_0}{(n'+1)^{t_0/2}(n'+1/2)} \simeq \frac{2}{t_0}\int_{u_\infty}^{u_0} \frac{du}{u_0} f(u) + c_2 = c_1/t_0 + c_2. \tag{C.2}$$

This allows us to determine the functional dependence of the leading eigenvalue λ_M on the parameter $t_0 \ll 1$. In the expression above, we have employed the asymptotic form of the right eigenvector r_n as $r_n = f(u_n)$ and replaced $(n+n'+1)$ with $\max\{(n+1/2)^{t_0/2}, (n'+1/2)^{t_0/2}\}$, which holds due to the smallness of the parameter t_0 and introduces a correction of the order of $O(t_0)$. By fitting the numerical results with the analytical expression (C.1), we find $c_1 \approx 1.38$ and $c_2 \approx 1.50$, yielding the result stated in Eq. (2.7).

It worth be pointed out that $\lambda_M \approx 1.38/t_0$ lies within the boundary of the Perron–Frobenius inequality,

$$\lambda_M \leqslant \max_n \sum_{n'=0}^{n_{\max}} M_{nn'} \simeq \frac{2}{t_0}. \tag{C.3}$$

Next, we consider the case of $\mathcal{N} = 0$, corresponding to strong spin-orbit

coupling characterized by the matrix $M_{nn'}(\ln n_{\max})$. To determine the functional dependence of λ_M on the matrix size $n_{\max}$, we can make use of an approximation $\ln(n+n'+1) \to \ln(\max n + 1/2, n' + 1/2)$. This approximation unveils

$$\lambda_M = \sum_{n' \geqslant 0}^{n_{\max}} \frac{\ln(n_{\max}) - \ln(n'+1)}{n'+1/2} \frac{\Delta_{n'}}{\Delta_0} \simeq \int_{u_\infty}^{u_0} duuf(u) + c_2 \ln n_{\max}. \tag{C.4}$$

With the help of Eqs. (3.9) and (3.12) and using $\pi^2/(|\gamma_0|t_0) = \ln^2 n_{\max}$, we find the following dimensional fitting,

$$\lambda_M = c_1 \ln^2 n_{\max} + c_2 \ln n_{\max}. \tag{C.5}$$

Using the aforementioned expression to fit the numerical data, we find that $c_1 \approx 0.406$ and $c_2 \approx 1.57$. It is worth noting that $c_1 = 0.406$ satisfies the Perron-Frobenius inequality, as one can verify:

$$\lambda_M \leqslant \max_n \sum_{n'=0}^{n_{\max}} M_{nn'}(\ln n_{\max}) \simeq \frac{\ln^2 n_{\max}}{2}. \tag{C.6}$$

D The Local Density of States

In this appendix, we delve into the details of the calculation of the disorder-averaged pair correlation function of the local density of states. In our approach, the mesoscopic fluctuations of the local density of states can be described using Q-matrices, as outlined in previous works [76, 77],

$$\begin{aligned} K_2(E,E',\boldsymbol{r}) &= \langle \delta\rho(E,\boldsymbol{r})\delta\rho(E',\boldsymbol{r})\rangle = \langle \rho(E,\boldsymbol{r})\rho(E',\boldsymbol{r})\rangle - \langle \rho(E,\boldsymbol{r})\rangle\langle \rho(E',\boldsymbol{r})\rangle \\ &= \frac{\nu^2}{32} \operatorname{Re}\left[P^{\alpha_1\alpha_2}_{2,irr}(i\varepsilon_1, i\varepsilon_3) - P^{\alpha_1\alpha_2}_{2,irr}(i\varepsilon_1, i\varepsilon_4)\right]. \end{aligned}$$

Here $\alpha_1 \neq \alpha_2$ are some fixed replica indices and analytical continuation, $i\varepsilon_{n_1} \to E + i0$, $i\varepsilon_{n_3} \to E' + i0$, $i\varepsilon_{n_4} \to E' - i0$, is assumed. $P^{\alpha_1\alpha_2}_{2,irr}(i\varepsilon_n, i\varepsilon_m)$ is the irreducible part of bilinear in Q operator,

$$P^{\alpha_1\alpha_2}_2 = \langle \operatorname{sp} Q^{\alpha_1\alpha_1}_{nn} \operatorname{sp} Q^{\alpha_2\alpha_2}_{mm} - 2 \operatorname{sp} Q^{\alpha_1\alpha_2}_{nm} Q^{\alpha_2\alpha_1}_{mn} \rangle. \tag{D.1}$$

To find mesoscopic fluctuations of the local density of states, we approximate $P^{\alpha_1\alpha_2}_{2,irr}(i\varepsilon_n, i\varepsilon_m)$ as

$$P^{\alpha_1\alpha_2}_{2,irr} \simeq -2\,\mathrm{sp}\langle (R^{-1}WR)^{\alpha_1\alpha_2}_{nm}(R^{-1}WR)^{\alpha_2\alpha_1}_{mn}\rangle. \tag{D.2}$$

Using Eq. (A.18), we find the following expression

$$\begin{aligned} P_2(i\varepsilon, i\varepsilon') = -\frac{32(1+\mathcal{N})}{g}\left[1 - \frac{\varepsilon}{\sqrt{\varepsilon^2+\Delta^2}}\frac{\varepsilon'}{\sqrt{\varepsilon'^2+\Delta^2}}\right] \\ \times \int \frac{d^2\boldsymbol{q}}{(2\pi)^2}\frac{D}{Dq^2 + \sqrt{\varepsilon^2+\Delta^2} + \sqrt{\varepsilon'^2+\Delta^2}}, \end{aligned} \tag{D.3}$$

that works for all signs of ε and ε'. We point out that this expression is only valid under the assumption (4.3), when energy dependence of the spectral gap function Δ_ε can be neglected. Then for $K_2(E, E', \boldsymbol{r})$, where $E, E' \gg \Delta$, we find the following lengthy expression,

$$\begin{aligned} K_2 = \frac{\nu^2(1+\mathcal{N})}{g}\sum_{s=\pm} s\left(1 + \frac{sEE'}{\sqrt{E^2-\Delta^2}\sqrt{E'^2-\Delta^2}}\right) \\ \times \mathrm{Re}\int_q \frac{D}{Dq^2 + i\sqrt{E^2-\Delta^2} - is\sqrt{E'^2-\Delta^2}}. \end{aligned} \tag{D.4}$$

Clearly, when $E = E'$, we obtain Eq. (4.4).

We now turn to the analysis of mesoscopic fluctuations in the local density of states at different energies $E \neq E'$. It is important to note that when the energies E and E' are close to each other, the pair correlation function $K_2(E, E', \boldsymbol{r})$ only exhibits slight differences compared to the case where the energies coincide, $K_2(E, E, \boldsymbol{r})$. Therefore, our focus is on energies that are well-separated from each other. Let's consider the case where $E' = E + \omega$, with ω being significantly larger than E. By expanding Equation (D.4) in terms of the small argument $E/\omega \ll 1$ and performing the integration with respect to momentum $\boldsymbol{q}$, we obtain Equation (4.7).

E The One-Loop Action for Fluctuastions

To determine the renormalized propagator, we begin by deriving an expression for quadratic fluctuations around the saddle point solution in various channels.

This can be done conveniently using the approach described in App. A. Only this time, one needs to take into account the inclusion of quartic terms as well. After some algebra, the answer can be succinctly written as follows

$$S_{\sigma}^{(2)}+S_{\rm int}^{c,(2)}=-\frac{g}{4}\sum_{\substack{r=0,3\\ j=1,2,3}}\sum_{\alpha\beta}\sum_{\varepsilon,\varepsilon'>0}\int_{q}[\mathcal{D}_{q}^{(0)}(i\varepsilon,i\varepsilon')]^{-1}\mathbf{\Phi}_{\varepsilon,-\varepsilon'}^{\alpha\beta,(r,j)}(\boldsymbol{q})\cdot\bar{\mathbf{\Phi}}_{-\varepsilon',\varepsilon}^{\beta\alpha,(r,j)}(-\boldsymbol{q}),$$

$$\begin{aligned}S_{\rm int}^{\sigma,(2)}=-4\pi T\Gamma_{s}\sum_{\alpha,n}\sum_{r=0,3}\int_{q}\sum_{\varepsilon_{1},\varepsilon_{2}>0}\boldsymbol{X}_{n}^{(r,0)}(\varepsilon_{1},\varepsilon_{2})\cdot\mathbf{\Phi}_{\varepsilon_{1},-\varepsilon_{2}}^{\alpha\alpha,(r,0)}(\boldsymbol{q})\\ \times\sum_{\varepsilon_{3},\varepsilon_{4}>0}[\boldsymbol{X}_{n}^{(r,0)}(\varepsilon_{4},\varepsilon_{3})]^{*}\cdot\bar{\mathbf{\Phi}}_{-\varepsilon_{4},\varepsilon_{3}}^{\alpha\alpha,(r,0)}(-\boldsymbol{q}),\end{aligned}$$

$$\begin{aligned}S_{\rm int}^{\rho,(2)}=-4\pi T\Gamma_{t}\sum_{\alpha,n}\sum_{\substack{r=0,3\\ j=1,2,3}}\int_{q}\sum_{\varepsilon_{1},\varepsilon_{2}>0}\boldsymbol{X}_{n}^{(r,j)}(\varepsilon_{1},\varepsilon_{2})\cdot\mathbf{\Phi}_{\varepsilon_{1},-\varepsilon_{2}}^{\alpha\alpha,(r,j)}(\boldsymbol{q})\\ \times\sum_{\varepsilon_{3},\varepsilon_{4}>0}[\boldsymbol{X}_{n}^{(r,j)}(\varepsilon_{4},\varepsilon_{3})]^{*}\cdot\bar{\mathbf{\Phi}}_{-\varepsilon_{4},\varepsilon_{3}}^{\alpha\alpha,(r,j)}(-\boldsymbol{q}),\end{aligned}$$

$$\begin{aligned}\hat{S}_{\rm int}^{c,(2)}=-4\pi T\Gamma_{c}\sum_{\alpha,n}\sum_{r=0,3}\int_{q}\left(1-\frac{(2\pi)^{2}\delta(\boldsymbol{q})\delta_{n0}}{V}\right)\sum_{\varepsilon_{1},\varepsilon_{2}>0}\boldsymbol{Y}_{n}^{(r)}(\varepsilon_{1},\varepsilon_{2})\cdot\mathbf{\Phi}_{\varepsilon_{1},-\varepsilon_{2}}^{\alpha\alpha,(r,0)}(\boldsymbol{q})\\ \times\sum_{\varepsilon_{3},\varepsilon_{4}>0}[\boldsymbol{Y}_{n}^{(r)}(\varepsilon_{4},\varepsilon_{3})]^{*}\cdot\bar{\mathbf{\Phi}}_{-\varepsilon_{4},\varepsilon_{3}}^{\alpha\alpha,(r,0)}(-\boldsymbol{q}).\end{aligned}\tag{E.1}$$

Here the vector fields read as

$$\boldsymbol{X}_n^{(0,j)}(\varepsilon,\varepsilon') = \begin{pmatrix} \cos\frac{\theta_\varepsilon+m_{0j}\theta_{\varepsilon'}}{2}(m_{0j}\delta_{\omega_n,\varepsilon+\varepsilon'}+\delta_{-\omega_n,\varepsilon+\varepsilon'}) \\ \sin\frac{\theta_\varepsilon-m_{0j}\theta_{\varepsilon'}}{2}(m_{0j}\delta_{-\omega_n,\varepsilon-\varepsilon'}+\delta_{\omega_n,\varepsilon-\varepsilon'}) \end{pmatrix}, \tag{E.2}$$

$$\boldsymbol{X}_n^{(3,j)}(\varepsilon,\varepsilon') = \begin{pmatrix} \cos\frac{\theta_\varepsilon+m_{0j}\theta_{\varepsilon'}}{2}(m_{3j}\delta_{\omega_n,\varepsilon+\varepsilon'}+\delta_{-\omega_n,\varepsilon+\varepsilon'}) \\ i\sin\frac{\theta_\varepsilon-m_{0j}\theta_{\varepsilon'}}{2}(m_{3j}\delta_{-\omega_n,\varepsilon-\varepsilon'}+\delta_{\omega_n,\varepsilon-\varepsilon'}) \end{pmatrix}, \tag{E.3}$$

$$\boldsymbol{Y}_n^{(0)}(\varepsilon,\varepsilon') = 2\begin{pmatrix} \cos\frac{\theta_{\varepsilon'}}{2}\sin\frac{\theta_\varepsilon}{2}\delta_{-\omega_n,\varepsilon+\varepsilon'}-\cos\frac{\theta_\varepsilon}{2}\sin\frac{\theta_{\varepsilon'}}{2}\delta_{\omega_n,\varepsilon+\varepsilon'} \\ \cos\frac{\theta_{\varepsilon'}}{2}\cos\frac{\theta_\varepsilon}{2}\delta_{\omega_n,\varepsilon-\varepsilon'}-\sin\frac{\theta_\varepsilon}{2}\sin\frac{\theta_{\varepsilon'}}{2}\delta_{-\omega_n,\varepsilon-\varepsilon'} \end{pmatrix}, \tag{E.4}$$

$$\boldsymbol{Y}_n^{(3)}(\varepsilon,\varepsilon') = 2\begin{pmatrix} -i\cos\frac{\theta_{\varepsilon'}}{2}\sin\frac{\theta_\varepsilon}{2}\delta_{-\omega_n,\varepsilon+\varepsilon'}-i\cos\frac{\theta_\varepsilon}{2}\sin\frac{\theta_{\varepsilon'}}{2}\delta_{\omega_n,\varepsilon+\varepsilon'} \\ \cos\frac{\theta_{\varepsilon'}}{2}\cos\frac{\theta_\varepsilon}{2}\delta_{\omega_n,\varepsilon-\varepsilon'}+\sin\frac{\theta_\varepsilon}{2}\sin\frac{\theta_{\varepsilon'}}{2}\delta_{-\omega_n,\varepsilon-\varepsilon'} \end{pmatrix}. \tag{E.5}$$

Finally, fields associated with W are defined in the main text, see (5.2).

The inverse of the operator $\hat{A}_{r,j}(q)$ defined in Eq. (5.3) can be found using perturbation theory. Indeed, for two invertible operators such that their sum is also an invertible operator, as α tends to 0, we can estimate

$$(\hat{A}+\alpha\hat{B})^{-1} \simeq \hat{A}^{-1} - \alpha\hat{A}^{-1}\hat{B}\hat{A}^{-1} + \ldots, \quad \alpha \to 0. \tag{E.6}$$

This brings us to Eq. (5.4), where we have defined

$$\hat{X}_{bb'}^{(r,j)}(\varepsilon_1,\varepsilon_2;\varepsilon_3,\varepsilon_4) \equiv \sum_n X_{n,b}^{(r,j)}(\varepsilon_1,\varepsilon_2)[X_{n,b'}^{(r,j)}(\varepsilon_4,\varepsilon_3)]^*, \tag{E.7}$$

$$\hat{Y}_{bb'}^{(r)}(\varepsilon_1,\varepsilon_2;\varepsilon_3,\varepsilon_4) \equiv \sum_n Y_{n,b}^{(r)}(\varepsilon_1,\varepsilon_2)[Y_{n,b'}^{(r)}(\varepsilon_4,\varepsilon_3)]^*. \tag{E.8}$$

F The Modified Usadel Equation

To find the renormalized equations for Δ_ε and Z_ε, one must obtain the effective action by averaging the fluctuation correction. This is done like the follows,

$$S_{\text{eff}}[\theta] = -\ln\int \mathcal{D}W \exp(-S_{\text{fl}}[\theta,W]). \tag{F.1}$$

Since we have already found the expression for the correlation of fields Φ, further computations are, although extensive, pretty straightforward. They yield

$$\langle S^{\sigma,(2)}_{\rm int}\rangle = -\frac{32\pi T N_r}{g}\mathcal{N}\Gamma_t \sum_{\varepsilon_1,\varepsilon_2>0}(\sin\theta_{\varepsilon_1}\sin\theta_{\varepsilon_2}+1)\int_q \mathcal{D}^{(0)}_q(i\varepsilon_1,i\varepsilon_2)+$$
$$+N_r\left(\frac{8\pi T\Gamma_t}{g}\right)^2 \sum_{\substack{r=0,3\\ j\neq 0}}\int_q \sum_{\varepsilon_i>0}\sum_{b,b'=1,2}\mathcal{D}^{(0)}_q(i\varepsilon_1,i\varepsilon_2)$$
$$\times\mathcal{D}^{(0)}_q(i\varepsilon_3,i\varepsilon_4)[\hat{X}^{(r,j)}_{bb'}(\varepsilon_1,\varepsilon_2;\varepsilon_3,\varepsilon_4)]^*\hat{X}^{(r,j)}_{bb'}(\varepsilon_1,\varepsilon_2;\varepsilon_3,\varepsilon_4) \tag{F.2}$$

for the triplet channel. For the singlet we find

$$\langle S^{\rho,(2)}_{\rm int}\rangle = \frac{32\pi T N_r}{g}\Gamma_s \sum_{\varepsilon_1,\varepsilon_2>0}(\sin\theta_{\varepsilon_1}\sin\theta_{\varepsilon_2}-1)\int_q \mathcal{D}^{(0)}_q(i\varepsilon_1,i\varepsilon_2)+$$
$$+N_r\left(\frac{8\pi T}{g}\right)^2\Gamma_s\sum_{r=0,3}\int_q\sum_{\varepsilon_i>0}\sum_{b,b'=1,2}\mathcal{D}^{(0)}_q(i\varepsilon_1,i\varepsilon_2)\mathcal{D}^{(0)}_q(i\varepsilon_3,i\varepsilon_4)[\hat{X}^{(r,0)}_{bb'}(\varepsilon_1,\varepsilon_2;\varepsilon_3,\varepsilon_4)]^*$$
$$\left[\Gamma_s\hat{X}^{(r,0)}_{bb'}(\varepsilon_1,\varepsilon_2;\varepsilon_3,\varepsilon_4)+\Gamma_c\left(\hat{Y}^{(r)}_{bb'}(\varepsilon_1,\varepsilon_2;\varepsilon_3,\varepsilon_4)-\frac{(2\pi)^2\delta(\boldsymbol{q})}{V}Y^{(r)}_{0,b}(\varepsilon_1,\varepsilon_2)[Y^{(r)}_{0,b'}(\varepsilon_4,\varepsilon_3)]^*\right)\right]. \tag{F.3}$$

Finally, the Cooper channel reads

$$\langle\hat{S}^{c,(2)}_{\rm int}\rangle = -\frac{32\pi T N_r}{g}\Gamma_c\left(2\int_q\sum_{\varepsilon_1,\varepsilon_2}\mathcal{D}^{(0)}_q(i\varepsilon_1,i\varepsilon_2)-\sum_{\varepsilon}\frac{2-\sin^2\theta_\varepsilon}{V}\mathcal{D}^{(0)}_{q=0}(i\varepsilon,i\varepsilon)\right)+$$
$$+N_r\left(\frac{8\pi T}{g}\right)^2\Gamma_c\sum_{r=0,3}\int_q\sum_{\varepsilon_i>0}\sum_{b,b'=1,2}\mathcal{D}^{(0)}_q(i\varepsilon_1,i\varepsilon_2)\mathcal{D}^{(0)}_q(i\varepsilon_3,i\varepsilon_4)$$
$$\times\left(\hat{Y}^{(r)}_{bb'}(\varepsilon_1,\varepsilon_2;\varepsilon_3,\varepsilon_4)-\frac{(2\pi)^2\delta(\boldsymbol{q})}{V}Y^{(r)}_{0,b}(\varepsilon_1,\varepsilon_2)[Y^{(r)}_{0,b'}(\varepsilon_4,\varepsilon_3)]^*\right)^*$$
$$\left[\Gamma_s\hat{X}^{(r,0)}_{bb'}(\varepsilon_1,\varepsilon_2;\varepsilon_3,\varepsilon_4)+\Gamma_c\left(\hat{Y}^{(r)}_{bb'}(\varepsilon_1,\varepsilon_2;\varepsilon_3,\varepsilon_4)-\frac{(2\pi)^2\delta(\boldsymbol{q})}{V}Y^{(r)}_{0,b}(\varepsilon_1,\varepsilon_2)[Y^{(r)}_{0,b'}(\varepsilon_4,\varepsilon_3)]^*\right)\right]. \tag{F.4}$$

By differentiating these expressions with respect to the spectral angle θ_ε and setting the result equal to zero, we obtain equations (5.5) and (5.6). We note that Δ_ε and Z_ε correspond to the solutions of the Usadel equation in the form

$$-|\varepsilon| Z_\varepsilon \sin\theta_\varepsilon + \Delta_\varepsilon \cos\theta_\varepsilon = 0. \tag{F.5}$$

To complete the picture, we provide the exact expressions for the functions introduced in Eqs. (5.5), (5.6).

$$\Pi^{(t)}(|\omega_n|, q) = \frac{16\pi T}{g} \sum_{\varepsilon_1,\varepsilon_2>0} \mathcal{D}_q^{(0)}(i\varepsilon_1, i\varepsilon_2) \Big[\delta_{\varepsilon_1+\varepsilon_2,|\omega_n|}(1+\cos(\theta_1-\theta_2)) + \delta_{|\varepsilon_1-\varepsilon_2|,|\omega_n|}(1-\cos(\theta_1+\theta_2)) \Big] \tag{F.6}$$

$$\Pi^{(s)}(|\omega_n|, q) = \frac{16\pi T}{g} \sum_{\varepsilon_1,\varepsilon_2>0} \mathcal{D}_q^{(0)}(i\varepsilon_1, i\varepsilon_2) \Big[\delta_{\varepsilon_1+\varepsilon_2,|\omega_n|}(1+\cos(\theta_1+\theta_2)) + \delta_{|\varepsilon_1-\varepsilon_2|,|\omega_n|}(1-\cos(\theta_1-\theta_2)) \Big] \tag{F.7}$$

$$\Pi_{\parallel}^{(c)}(|\omega_n|, q) = \frac{16\pi T}{g} \sum_{\varepsilon_1,\varepsilon_2>0} \mathcal{D}_q^{(0)}(i\varepsilon_1, i\varepsilon_2) \Big[\delta_{\varepsilon_1+\varepsilon_2,|\omega_n|}(1-\cos(\theta_1-\theta_2)) + \delta_{|\varepsilon_1-\varepsilon_2|,|\omega_n|}(1+\cos(\theta_1+\theta_2)) \Big] \tag{F.8}$$

$$\Pi_{\perp}^{(c)}(|\omega_n|, q) = \frac{16\pi T}{g} \sum_{\varepsilon_1,\varepsilon_2>0} \mathcal{D}_q^{(0)}(i\varepsilon_1, i\varepsilon_2) \Big[\delta_{\varepsilon_1+\varepsilon_2,|\omega_n|} + \delta_{|\varepsilon_1-\varepsilon_2|,|\omega_n|} \Big] \sin\theta_{\varepsilon_1} \sin\theta_{\varepsilon_2} \tag{F.9}$$

$$\Pi_{A}^{(c)}(|\omega_n|, q) = -\frac{8\pi T}{g} \sum_{\varepsilon_1,\varepsilon_2>0} \mathcal{D}_q^{(0)}(i\varepsilon_1, i\varepsilon_2) \Big[\delta_{\varepsilon_1+\varepsilon_2,|\omega_n|} \sin(\theta_{\varepsilon_1}+\theta_{\varepsilon_2}) - \delta_{|\varepsilon_1-\varepsilon_2|,|\omega_n|} \sin\theta_{\varepsilon_1} \sin\theta_{\varepsilon_2} \operatorname{sgn}(\varepsilon_1-\varepsilon_2) \Big] \tag{F.10}$$